A SECOND-ORDER STABILIZATION METHOD FOR LINEARIZING AND DECOUPLING NONLINEAR PARABOLIC SYSTEMS

BUYANG LI*, YUKI UEDA†, AND GUANYU ZHOU‡

Abstract. A new time discretization method for strongly nonlinear parabolic systems is constructed by combining the fully explicit two-step backward difference formula and a second-order stabilization of wave type. The proposed method linearizes and decouples a nonlinear parabolic system at every time level, with second-order consistency error. The convergence of the proposed method is proved by combing energy estimates for evolution equations of parabolic and wave types, and the generating function technique that is popular in studying ordinary differential equations. Several numerical examples are provided to support the theoretical result.

Key words. nonlinear parabolic system, stabilization, linearization, decoupling, convergence

AMS subject classifications. 65M12, 35K61, 53E10

1. Introduction.

Strongly nonlinear parabolic systems arise in a variety of applications, including optimal transportation problems [29, 33], large deviation of diffusion processes [9, 18], models for porous media [25, 32], and image processing [23, 31]. In differential geometry, the geometric gradient flow associated to a curvature functional on a manifold is naturally a strongly nonlinear parabolic system [7, 28].

An example of strongly nonlinear parabolic systems is the L^2 gradient flow associated to an energy functional

$$E[\boldsymbol{u}] = \int_\Omega F(\boldsymbol{u}, \nabla \boldsymbol{u}) \mathrm{d}x, \quad \text{with a given function } F : \mathbb{R}^m \times \mathbb{R}^{d\times m} \to \mathbb{R}, \tag{1.1}$$

where $\boldsymbol{u} = (u_1, \dots, u_m)$ is a function defined on a bounded domain $\Omega \subset \mathbb{R}^d$ with $d \in \{1, 2, 3\}$, and

$$\nabla \boldsymbol{u} = (\nabla u_1, \dots, \nabla u_m) \in L^\infty(\Omega)^{d\times m},$$

with each ∇u_j denoting a d-dimensional column vector-valued function. The L^2 gradient flow of (1.1) is the solution of the following initial-boundary value problem

$$\kappa(\boldsymbol{u}, \nabla \boldsymbol{u}) \frac{\partial \boldsymbol{u}}{\partial t} = -E'[\boldsymbol{u}] \quad \text{in } \Omega \times (0, T] \tag{1.2}$$

where $\kappa(\boldsymbol{u}, \nabla \boldsymbol{u})$ is a positive weight function and $E'[\boldsymbol{u}]$ denotes the Frechet derivative of the energy functional $E[\boldsymbol{u}]$, given by

$$E'[\boldsymbol{u}] = -\nabla \cdot (DF(\boldsymbol{u}, \nabla \boldsymbol{u})) + D_{\boldsymbol{u}} F(\boldsymbol{u}, \nabla \boldsymbol{u});$$

the notations $D_{\boldsymbol{u}}$ and D stand for differentiation in $\boldsymbol{u}$ and $\nabla \boldsymbol{u}$, respectively.

Examples of (1.2) include (but not limited to):

*Department of Applied Mathematics, The Hong Kong Polytechnic University, Hung Hom, Hong Kong. The research of B. Li was partially supported by an internal grant of The Hong Kong Polytechnic University (project code: ZZKQ). E-mail address: buyang.li@polyu.edu.hk

†Department of Applied Mathematics, The Hong Kong Polytechnic University, Hung Hom, Hong Kong. The research of Y. Ueda was partially supported by the Hong Kong RGC grant 15300817.

Current address: Waseda Research Institute for Science and Engineering, Faculty of Science and Engineering, Waseda University, Japan. E-mail address: yuki.ueda@aoni.waseda.jp

‡Corresponding author. Institute of Fundamental and Frontier Sciences, University of Electronic Science and Technology of China, Chengdu, China. E-mail address: koolewind@gmail.com

1. *Regularized total variation flow* (cf. [10])

$$\frac{\partial u}{\partial t} = \nabla \cdot \left(\frac{\nabla u}{\sqrt{\varepsilon^2 + |\nabla u|^2}} \right) - \lambda (u - g), \tag{1.3}$$

which is a noise removal model in image processing (as a regularized approximation to the total variation model of [27]). This is the gradient flow of the energy functional

$$E[u] = \int_\Omega \sqrt{\varepsilon^2 + |\nabla u|^2} \mathrm{d}x + \frac{\lambda}{2} \int_\Omega |u - g|^2 \mathrm{d}x$$

with $\kappa = 1$, where g is a given function representing the observed image with noise, while ε and λ are constant parameters.

2. *Mean curvature flow of graphs* (cf. [13]) :

$$\sqrt{1 + |\nabla u|^2} \frac{\partial u}{\partial t} = \nabla \cdot \left(\frac{\nabla u}{\sqrt{1 + |\nabla u|^2}} \right), \tag{1.4}$$

which is the gradient flow of the surface area functional

$$E[u] = \int_\Omega \sqrt{1 + |\nabla u|^2} \mathrm{d}x$$

with $\kappa = \sqrt{1 + |\nabla u|^2}$. On a bounded domain $\Omega \subset \mathbb{R}^2$, the surface described by the graph $\{(x, u(x)) : x \in \Omega\}$ evolves to the minimal surface under a given boundary condition.

3. *Re-parameterized curve shortening flow* (cf. [5, 8]):

$$\left| \frac{\partial \boldsymbol{u}}{\partial s} \right|^2 \frac{\partial \boldsymbol{u}}{\partial t} = \frac{\partial^2 \boldsymbol{u}}{\partial s^2} \qquad (s, t) \in [0, 2\pi] \times (0, T] \tag{1.5}$$

with the periodic boundary condition, which describes the evolution of a closed curve $\boldsymbol{u}(\cdot, t) : [0, 2\pi] \to \mathbb{R}^2$ on the plane with normal velocity being the curvature on the curve. This is the gradient flow of

$$E[\boldsymbol{u}] = \int_0^{2\pi} \left| \frac{\partial \boldsymbol{u}}{\partial s} \right|^2 \mathrm{d}s$$

with weight $\kappa = \left| \frac{\partial \boldsymbol{u}}{\partial s} \right|^2$. This curve flow differs from the standard curve shortening flow by a tangential velocity (equivalent to a re-parametrization of the curve) which does not change the shape of the curve.

For all the examples mentioned above, the function $F : \mathbb{R}^m \times \mathbb{R}^{d \times m} \to \mathbb{R}$ is smooth and strictly convex in the second argument, i.e. the Hessian matrix $D_{kl} D_{ij} F(\mu, \xi)$ is a positive definite tensor at any point $(\mu, \xi) \in \mathbb{R}^d \times \mathbb{R}^{d \times m}$. This makes problem (1.2) essentially parabolic. The equations are strongly nonlinear (with nonlinearity containing $\nabla \boldsymbol{u}$) and coupled in the case $m \geq 2$. This makes numerical analysis challenging.

If $DF(\boldsymbol{u}, \nabla \boldsymbol{u})$ depends linearly on $\nabla \boldsymbol{u}$ and $\kappa(\boldsymbol{u}, \nabla \boldsymbol{u}) = 1$, then (1.2) reduces to a quasilinear parabolic equation

$$\frac{\partial \boldsymbol{u}}{\partial t} - \nabla \cdot (2a(\boldsymbol{u}) \nabla \boldsymbol{u}) + \boldsymbol{f}(\boldsymbol{u}, \nabla \boldsymbol{u}) = 0 \quad \text{in } \Omega \times (0, T], \tag{1.6}$$

for a vector-valued function $\boldsymbol{f}(\boldsymbol{u},\nabla\boldsymbol{u})$ and some symmetric tensor-valued function $a(\boldsymbol{u})$ which does not depend on $\nabla\boldsymbol{u}$. Error estimates for time discretization of such quasilinear parabolic equations have been established for many different methods, including Runge–Kutta methods [21], A(θ)-stable multistep methods [20], implicit–explicit BDF methods [1, 2], and semi-implicit BDF methods for the SAV formulation [30].

If $DF(\boldsymbol{u},\nabla\boldsymbol{u})$ and $\kappa(\boldsymbol{u},\nabla\boldsymbol{u})$ depend nonlinearly on $\nabla\boldsymbol{u}$, especially when the eigenvalues of $D_{kl}D_{ij}F(\mu,\xi)$ do not have positive upper and lower bounds for $(\mu,\xi)\in\mathbb{R}^m\times\mathbb{R}^{d\times m}$, then numerical analysis for (1.2) is more difficult. Typically, it requires proving $W^{1,\infty}$-boundedness of numerical solutions in order to rule out the possibility of degeneracy. In this case, very few works have been done in the literature. As far as we know, the implicit Euler method was considered in [10] for a regularized total variation flow problem by using energy techniques; implicit Runge–Kutta methods were considered in [24] and [15] using sectorial operator techniques and the maximal L^p-regularity approach, respectively. Besides fully implicit schemes, a linearly implicit Euler method was proved to be convergent [17] for the specific minimal surface flow equation. Overall, when $DF(\boldsymbol{u},\nabla\boldsymbol{u})$ and $\kappa(\boldsymbol{u},\nabla\boldsymbol{u})$ depend nonlinearly on $\nabla\boldsymbol{u}$, rigorous analysis has only been done for either nonlinearly implicit schemes or first-order linearly implicit schemes.

In this article, we introduce a *second-order* stabilization method to *linearize* and *decouple* the strongly nonlinear parabolic system (1.2) at every time level. In particular, the components u_j, $j=1\dots,m$ of the solution $\boldsymbol{u}=(u_1,\dots,u_m)^\top$ can be solved in parallel. For simplicity, we present the method and convergence analysis for the case $F=F(\nabla\boldsymbol{u})$ and $\kappa=\kappa(\nabla\boldsymbol{u})$, and restrict our attention to the Dirichlet boundary condition. In this case, problem (1.2) is equivalent to the following nonlinear initial-boundary value problem:

$$\begin{cases}\kappa(\nabla\boldsymbol{u})\dfrac{\partial\boldsymbol{u}}{\partial t}=\nabla\cdot A(\nabla\boldsymbol{u}) & \text{in } \Omega\times(0,T],\\ \qquad\quad \boldsymbol{u}=\boldsymbol{g} & \text{on } \partial\Omega\times(0,T],\\ \qquad \boldsymbol{u}|_{t=0}=\boldsymbol{u}_0 & \text{in } \Omega,\end{cases}\tag{1.7}$$

where $A(\xi)=(D_{ij}F(\xi))_{d\times m}$ is a nonlinear matrix-valued function of $\xi=(\xi_{ij})\in\mathbb{R}^{d\times m}$ with D_{ij} denoting differentiation with respect to ξ_{ij}, and

$$\nabla\cdot A(\nabla\boldsymbol{u}):=\Big(\sum_{i=1}^d\partial_iD_{i1}F(\nabla\boldsymbol{u}),\sum_{i=1}^d\partial_iD_{i2}F(\nabla\boldsymbol{u}),\dots,\sum_{i=1}^d\partial_iD_{im}F(\nabla\boldsymbol{u})\Big)^\top.$$

The simplifications $F=F(\nabla\boldsymbol{u})$ and $\kappa=\kappa(\nabla\boldsymbol{u})$ keep the essential nonlinear structure and the mathematical difficulties of the problem, i.e. (1.7) only differs from (1.2) by low-order terms. Hence, both the numerical method and convergence analysis presented in this paper can be carried over to the general case with $F=F(\boldsymbol{u},\nabla\boldsymbol{u})$ and $\kappa=\kappa(\boldsymbol{u},\nabla\boldsymbol{u})$.

Our method is inspired by [22], in which a first-order stabilization method

$$\frac{\boldsymbol{u}_n-\boldsymbol{u}_{n-1}}{\tau}=\Delta\boldsymbol{a}(\boldsymbol{u}_{n-1})+\frac{1}{\alpha}\big(\Delta\boldsymbol{u}_n-\Delta\boldsymbol{u}_{n-1}\big),\tag{1.8}$$

was proposed to decouple the weakly nonlinear parabolic system

$$\frac{\partial\boldsymbol{u}}{\partial t}=\Delta\,\boldsymbol{a}(\boldsymbol{u}).\tag{1.9}$$

Here, $\boldsymbol{u}_n$ is an approximation to $\boldsymbol{u}(t_n)$ at time levels $t_n = n\tau$, $n = 1, \dots, N$, with stepsize $\tau = T/N$. The method was proved to be first-order convergent for sufficiently small stabilization parameter α.

We consider the following method for the strongly nonlinear parabolic system (1.7):

$$\begin{cases} \kappa(\nabla I_\tau \boldsymbol{u}_n)\delta_\tau \boldsymbol{u}_n - \dfrac{1}{\alpha}\Delta \boldsymbol{u}_n = \nabla \cdot A(\nabla I_\tau \boldsymbol{u}_n) - \dfrac{1}{\alpha}\Delta I_\tau \boldsymbol{u}_n & \text{in } \Omega, \\ \boldsymbol{u}_n = \boldsymbol{g}(t_n) & \text{on } \partial\Omega, \end{cases} \tag{1.10}$$

where

$$\delta_\tau \boldsymbol{u}_n = \frac{1}{\tau}\left(\frac{3}{2}\boldsymbol{u}_n - 2\boldsymbol{u}_{n-1} + \frac{1}{2}\boldsymbol{u}_{n-2}\right) \quad \text{and} \quad I_\tau \boldsymbol{u}_n = 2\boldsymbol{u}_{n-1} - \boldsymbol{u}_{n-2},$$

denote second-order backward differentiation and extrapolation formulas, respectively. Clearly, the method (1.10) linearizes the system and decouples the components of $\boldsymbol{u}$. Hence, at every time level, the components u_j, $j = 1 \dots, m$ of the solution $\boldsymbol{u} = (u_1, \dots, u_m)^\top$ can be solved in parallel.

The stability of this linearization and decoupling would be guaranteed by the second-order stabilization term

$$\frac{1}{\alpha}\big(\Delta \boldsymbol{u}_n - 2\Delta \boldsymbol{u}_{n-1} + \Delta \boldsymbol{u}_{n-2}\big),$$

which has second-order accuracy but leads to essential difficulties to error analysis because of the wave nature of this stabilization term (this term mimics $\frac{\tau^2}{\alpha}\partial_{tt}\Delta \boldsymbol{u}$). The wave nature of this stabilization term requires using different test functions and techniques in the convergence analysis. In particular, the error analysis for the first-order method (1.8) only requires testing the equation by the error $\boldsymbol{u}(t_n) - \boldsymbol{u}_n$, but the error analysis for the second-order method (1.10) requires testing the error equation by both $\boldsymbol{u}(t_n) - \boldsymbol{u}_n$ and $\boldsymbol{u}(t_n) - \boldsymbol{u}(t_{n-1}) - \boldsymbol{u}_n + \boldsymbol{u}_{n+1}$ and then combine the two results. Another difficulty of the error analysis is due to the strong nonlinear structure of the problem, which requires proving $W^{1,\infty}$-boundedness of numerical solutions in order to rule out the possibility of degeneracy. This is overcome by establishing H^2 and H^3 energy estimates for equations of the type (see Lemma 3.1)

$$\nabla \cdot Q_n \nabla \boldsymbol{e}_n + \frac{1}{\alpha}\big(\Delta \boldsymbol{e}_n - 2\Delta \boldsymbol{e}_{n-1} + \Delta \boldsymbol{e}_{n-2}\big) = \boldsymbol{f}_n, \quad n = 2, \dots, N, \tag{1.11}$$

where Q_n is an elliptic operator, and $\boldsymbol{e}_n = \boldsymbol{u}(t_n) - \boldsymbol{u}_n$ is the error of the numerical solution. Again, due to the wave nature of the stabilization term $\frac{1}{\alpha}\big(\Delta \boldsymbol{e}_n - 2\Delta \boldsymbol{e}_{n-1} + \Delta \boldsymbol{e}_{n-2}\big)$, the H^2 and H^3 energy estimates can hardly be established through multiplying the above equation by test functions. We overcome this difficulty by using the generating function technique (see Lemma 4.1) widely used in the community of ordinary differential equations, together with a perturbation argument which allows us to freeze Q_n at a fixed time level (when using the generating function technique).

The numerical methods and convergence analysis presented in this article are applicable not only to L^2 gradient flows but also to more general nonlinear parabolic systems. Two of such examples are given in Section 5.2, i.e., the generalized Newtonian fluid flow and a nonlinear parabolic system of non-divergence form.

2. Main results. For abbreviation, the inner products and norms of $L^2(\Omega)$, $L^2(\Omega)^m$ and $L^2(\Omega)^{d\times m}$ are all denoted by $(\cdot,\cdot)$ and $\|\cdot\|_{L^2}$, respectively. Similarly, the norms of the Sobolev spaces $W^{s,p}(\Omega)$, $W^{s,p}(\Omega)^m$ and $W^{s,p}(\Omega)^{d\times m}$ are all denoted by $\|\cdot\|_{W^{s,p}}$, with conventional abbreviation $\|\cdot\|_{H^s}=\|\cdot\|_{W^{s,2}}$.

2.1. Assumptions. We prove the stability and convergence of the proposed numerical method (1.10) under the following assumptions:

(A1) F is smooth and strictly convex, i.e. the Hessian tensor $D_{kl}D_{ij}F(\xi)$ is positive definite at any $\xi\in\mathbb{R}^{d\times m}$.

(A2) κ is smooth and positive, i.e.

$$\kappa(\nabla\boldsymbol{u}(x,t))>0\quad\text{for the exact solution }\boldsymbol{u}\text{ and }(x,t)\in\overline{\Omega}\times[0,T].$$

(A3) The domain Ω and the solution of (1.7) are sufficiently smooth.

(A4) The initial values $\boldsymbol{u}_0$ and $\boldsymbol{u}_1$ are given sufficiently accurately, i.e.

$$\|\boldsymbol{u}(t_0)-\boldsymbol{u}_0\|_{H^k}+\|\boldsymbol{u}(t_1)-\boldsymbol{u}_1\|_{H^k}\le C_0\tau^{2-\frac{k}{2}},\quad k=0,1,2,3,$$

where C_0 is some positive constant.

Indeed, assumptions (A1) and (A2) are true for all examples mentioned in Section 1. For the third example in Section 1 (re-parameterized curve shortening flow), we assume that the exact solution is a curve satisfying the non-degeneracy condition $|\partial_s\boldsymbol{u}(s,t)|>0$ for all $s\in[0,2\pi]$ and $t\in[0,T]$.

2.2. Consequences of assumptions. By using the integral form of the mean value theorem, it is straightforward to verify the following identity:

$$\begin{aligned}(A(\nabla\boldsymbol{u})-A(\nabla\boldsymbol{v}))\cdot\nabla\boldsymbol{w}&=\sum_{j,l=1}^{m}\sum_{i,k=1}^{d}B_{kl,ij}(\nabla\boldsymbol{u},\nabla\boldsymbol{v})\partial_k(u_l-v_l)\partial_i w_j\\&=:B(\nabla\boldsymbol{u},\nabla\boldsymbol{v})\nabla(\boldsymbol{u}-\boldsymbol{v})\cdot\nabla\boldsymbol{w},\end{aligned}\tag{2.1}$$

where $B(\nabla\boldsymbol{u},\nabla\boldsymbol{v})$ is a symmetric tensor with components $B_{kl,ij}(\nabla\boldsymbol{u},\nabla\boldsymbol{v})$ defined by

$$B_{kl,ij}(\xi,\eta)=\int_0^1 D_{kl}D_{ij}F((1-\theta)\xi+\theta\eta)\mathrm{d}\theta,\quad\forall\,\xi,\eta\in\mathbb{R}^{d\times m}.\tag{2.2}$$

Under assumptions (A1)-(A2), there exists an increasing function $\phi:\mathbb{R}_+\to\mathbb{R}_+$ such that the following two properties hold:

(P1) (Local Lipschitz continuity) The functions $\kappa(\xi)$, $A(\xi)$ and $B(\xi,\eta)$ satisfy

$$|\kappa(\xi)-\kappa(\eta)|\le\phi(r)|\xi-\eta|,\quad\forall\,\xi,\eta\in\mathbb{R}^{d\times m}\ \text{satisfying}\ |\xi|\le r\ \text{and}\ |\eta|\le r,$$

$$|A(\xi)-A(\eta)|\le\phi(r)|\xi-\eta|,\quad\forall\,\xi,\eta\in\mathbb{R}^{d\times m}\ \text{satisfying}\ |\xi|\le r\ \text{and}\ |\eta|\le r,$$

$$\begin{aligned}&|B(\xi_1,\eta_1)-B(\xi_2,\eta_2)|\le\phi(r)(|\xi_1-\xi_2|+|\eta_1-\eta_2|)\\&\qquad\forall\,\xi_1,\xi_2,\eta_1,\eta_2\in\mathbb{R}^{d\times m}\ \text{satisfying}\ |\xi_1|\le r,|\xi_2|\le r,|\eta_1|\le r,|\eta_2|\le r.\end{aligned}$$

(P2) (Local positivity) There exists a positive constant $\sigma>0$ such that

$$\kappa(\xi)\ge\kappa_*,\qquad\text{when }|\xi-\nabla\boldsymbol{u}(x,t)|\le3\sigma\text{ for some }(x,t)\in\Omega\times[0,T],$$

$$B(\xi,\eta)\zeta\cdot\zeta \geq \frac{1}{\phi(r)}|\zeta|^2, \quad \forall\,\zeta,\xi,\eta\in\mathbb{R}^{d\times m} \text{ satisfying } |\xi|\leq r \text{ and } |\eta|\leq r,$$

where κ_* is some positive constant.

2.3. Main result. The main theoretical result of this paper is the following theorem, which is proved in the next section.

Theorem 2.1. *Let $d\in\{1,2,3\}$. Under assumptions* (A1)–(A4)*, there exists a positive constant α_0 (independent of τ) such that when $\alpha\leq\alpha_0$ the numerical solutions given by* (1.10) *have the following error bound:*

$$\max_{2\leq n\leq N}\|\boldsymbol{u}_n-\boldsymbol{u}(t_n)\|_{H^s}\leq C\tau^{2-\frac{s}{2}}, \quad s=0,1,2,3, \tag{2.3}$$

$$\tau\sum_{n=2}^{k}\|(\boldsymbol{u}_n-\boldsymbol{u}_{n-1})/\tau\|_{H^3}^2\leq C. \tag{2.4}$$

The proof of Theorem 2.1 is presented in the next section.

3. Error estimation. For a sequence of functions v_n, $n=0,1,\dots,N$, we denote

$$P(v_n)=|v_n|^2+|2v_n-v_{n-1}|^2$$
$$Q(v_n)=|v_n-v_{n-1}|^2.$$

Then

$$\delta_\tau v_n\, v_n=\frac{1}{4\tau}|v_n-I_\tau v_n|^2+\frac{P(v_n)}{4\tau}-\frac{P(v_{n-1})}{4\tau}, \tag{3.1a}$$

$$\begin{aligned}\delta_\tau v_n(v_n-v_{n-1}) &= \frac{3}{2\tau}Q(v_n)-\frac{1}{2\tau}(v_{n-1}-v_{n-2})(v_n-v_{n-1})\\ &\geq \frac{Q(v_n)}{\tau}+\frac{Q(v_n)}{4\tau}-\frac{Q(v_{n-1})}{4\tau},\end{aligned} \tag{3.1b}$$

$$\begin{aligned}(v_n-I_\tau v_n)v_n &= (v_n-v_{n-1})v_n-(v_{n-1}-v_{n-2})v_n\\ &= \frac{Q(v_n)}{2}+\frac{1}{2}|v_n|^2-\frac{1}{2}|v_{n-1}|^2-(v_{n-1}-v_{n-2})v_n\\ &\geq \frac{Q(v_n)}{2}+\frac{1}{2}|v_n|^2-\frac{1}{2}|v_{n-1}|^2-\left(\frac{Q(v_{n-1})}{\ell}+\frac{\ell}{4}|v_n|^2\right),\end{aligned} \tag{3.1c}$$

$$(v_n-I_\tau v_n)(v_n-v_{n-1})=\frac{1}{2}|v_n-I_\tau v_n|^2+\frac{Q(v_n)}{2}-\frac{Q(v_{n-1})}{2}. \tag{3.1d}$$

Equality (3.1a) can be found in [19, eq. (2.3)]. The second equality in (3.1c) is also due to [19, eq. (2.3)], and the inequality in (3.1c) is due to Young's inequality. The equalities in (3.1b) and (3.1d) are due to the definitions of δ_τ and I_τ, respectively.

In the rest of this paper, we denote by C a generic positive constant which does not depend on the stepsize or time-levels.

3.1. Consistency and error equations. Note that the exact solution $\boldsymbol{u}(t_n)$ satisfies

$$\kappa(\nabla I_\tau\boldsymbol{u}(t_n))\,\delta_\tau\boldsymbol{u}(t_n)=\nabla\cdot A(\nabla I_\tau\boldsymbol{u}(t_n))$$

$$+\frac{1}{\alpha}(\Delta \boldsymbol{u}(t_n) - 2\Delta \boldsymbol{u}(t_{n-1}) + \Delta \boldsymbol{u}(t_{n-2})) + \boldsymbol{b}_n + \boldsymbol{d}_n \qquad (3.2)$$

with $\boldsymbol{b}_n$ and $\boldsymbol{d}_n$ denoting the truncation errors of time discretization, given by

$$\boldsymbol{b}_n = \kappa(\nabla I_\tau \boldsymbol{u}(t_n))\Big(\delta_\tau \boldsymbol{u}(t_n) - \frac{\partial \boldsymbol{u}}{\partial t}(t_n)\Big) + \big(\kappa(\nabla I_\tau \boldsymbol{u}(t_n)) - \kappa(\nabla \boldsymbol{u}(t_n))\big)\frac{\partial \boldsymbol{u}}{\partial t}(t_n),$$

$$\boldsymbol{d}_n = \nabla\cdot A(\nabla \boldsymbol{u}(t_n)) - \nabla\cdot A(\nabla I_\tau \boldsymbol{u}(t_n)) - \frac{1}{\alpha}(\Delta \boldsymbol{u}(t_n) - 2\Delta \boldsymbol{u}(t_{n-1}) + \Delta \boldsymbol{u}(t_{n-2})).$$

For a sufficiently smooth function v, it is well-known that

$$\Big\|\delta_\tau v(t_n) - \frac{\partial v}{\partial t}(t_n)\Big\|_{H^s} \le C\|\partial_{ttt} v\|_{C([0,T];H^s)}\tau^2, \qquad (3.4)$$

$$\|v(t_n) - I_\tau v(t_n)\|_{H^s} \le C\|\partial_{tt} v\|_{C([0,T];H^s)}\tau^2, \qquad (3.5)$$

where s can be any nonnegative integer. Hence, for a sufficiently smooth solution $\boldsymbol{u}$, the truncation errors satisfy

$$\|\boldsymbol{b}_n\|_{H^1} + \|\boldsymbol{d}_n\|_{H^1} \le C\tau^2. \qquad (3.6)$$

By subtracting (1.10) from (3.2), we see that the error function $\boldsymbol{e}_n = \boldsymbol{u}(t_n) - \boldsymbol{u}_n$ satisfies the following equation:

$$\begin{aligned}\kappa(\nabla I_\tau \boldsymbol{u}_n)\,\delta_\tau \boldsymbol{e}_n = &-(\kappa(\nabla I_\tau \boldsymbol{u}(t_n)) - \kappa(\nabla I_\tau \boldsymbol{u}_n))\delta_\tau \boldsymbol{u}(t_n)\\ &+ \nabla\cdot A(\nabla I_\tau \boldsymbol{u}(t_n)) - \nabla\cdot A(\nabla I_\tau \boldsymbol{u}_n)\\ &+ \frac{1}{\alpha}(\Delta \boldsymbol{e}_n - \Delta I_\tau \boldsymbol{e}_n) + \boldsymbol{b}_n + \boldsymbol{d}_n. \qquad (3.7)\end{aligned}$$

3.2. Induction assumption. For abbreviation, we denote

$$r = \|\boldsymbol{u}\|_{C([0,T];W^{1,\infty}(\Omega)^m)} + \sigma, \quad a = 1/\phi(r) \quad \text{and} \quad K = \phi(3r). \qquad (3.8)$$

In the error estimation, we first assume that the inequalities

$$\|\boldsymbol{e}_n\|_{W^{1,\infty}} \le \sigma, \quad \sum_{j=1}^{n}\|\boldsymbol{e}_j - \boldsymbol{e}_{j-1}\|_{W^{1,\infty}} \le 1, \qquad (3.9a)$$

$$\|\boldsymbol{e}_n\|_{H^1} \le \tau^{\frac{5}{4}} \quad \text{and} \quad \|\boldsymbol{e}_n\|_{H^3} \le \tau^{\frac{1}{4}} \qquad (3.9b)$$

hold for $0 \le n \le k-1$. Under this assumption, the following inequalities hold:

$$\|I_\tau \boldsymbol{e}_n\|_{W^{1,\infty}} = \|2\boldsymbol{e}_{n-1} - \boldsymbol{e}_{n-2}\|_{W^{1,\infty}} \le 3\sigma \quad \text{for } 2 \le n \le k, \qquad (3.10)$$

$$\|I_\tau \boldsymbol{u}_n\|_{W^{1,\infty}} = \|2\boldsymbol{u}_{n-1} - \boldsymbol{u}_{n-2}\|_{W^{1,\infty}} \le 3r \quad \text{for } 2 \le n \le k, \qquad (3.11)$$

and

$$\begin{aligned}\sum_{j=1}^{n}\|\boldsymbol{u}_j - \boldsymbol{u}_{j-1}\|_{W^{1,\infty}} &\le \sum_{j=1}^{n}\|\boldsymbol{u}(t_j) - \boldsymbol{u}(t_{j-1})\|_{W^{1,\infty}} + \sum_{j=1}^{n}\|\boldsymbol{e}_j - \boldsymbol{e}_{j-1}\|_{W^{1,\infty}}\\ &\le T\|\partial_t \boldsymbol{u}\|_{C([0,T];W^{1,\infty})} + 1 =: C_*. \qquad (3.12)\end{aligned}$$

Inequality (3.10) and (P2) imply that

$$\kappa(\nabla I_\tau \boldsymbol{u}_n) \ge \kappa_* \quad \text{for } 2 \le n \le k. \qquad (3.13)$$

We shall use these properties to prove that (3.9) also hold for $n = k$. Then, by mathematical induction, (3.9) holds for all $0 \le n \le N$.

3.3. An overview of the error analysis. In this subsection, we present an overview of the error analysis in the rest of this article, together with the motivation of the techniques we use.

We shall begin with the standard L^2-norm error estimate in Section 3.5, by testing the error equation (3.7) with $\boldsymbol{e}_n$. Since the second term on the right-hand side of (3.7) is fully explicit, its product with $\boldsymbol{e}_n$ needs to be controlled by using the stabilization term. However, the second-order stabilization term $\frac{1}{\alpha}(\Delta \boldsymbol{e}_n - \Delta I_\tau \boldsymbol{e}_n)$ is of wave type, which requires a test function in the form of $\boldsymbol{e}_n - \boldsymbol{e}_{n-1}$ instead of $\boldsymbol{e}_n$. This motivates us to test the error equation by $\boldsymbol{e}_n - \boldsymbol{e}_{n-1}$ in Section 3.5. The two estimates will be combined together, to yield discrete $L^\infty(0,T;L^2)$ and $L^2(0,T;H^1)$ error estimates. Due to the strong nonlinearities, we will obtain

$$
\begin{aligned}
&\max_{2\le n\le k} \|\boldsymbol{e}_n\|_{L^2}^2 + \tau \sum_{n=2}^{k} \|\nabla \boldsymbol{e}_n\|_{L^2}^2 \\
&\le C\tau^4 + C\sum_{n=1}^{k} \tau \|\nabla \boldsymbol{e}_{n-1}\|_{L^2}(\|\nabla \boldsymbol{e}_{n-1}\|_{L^4}^2 + \|\nabla \boldsymbol{e}_n\|_{L^4}^2),
\end{aligned}
$$

with an additional three-term product of errors on the right-hand side; see (3.27). In the derivation of this inequality, we would need to use the smallness of the error in the $W^{1,\infty}$-norm to control the nonlinearities. This is guaranteed by the induction assumption $\|\boldsymbol{e}_n\|_{H^3} \le \tau^{\frac14}$ in (3.9) (for $n \le k-1$) and the Sobolev embedding $H^3 \hookrightarrow W^{1,\infty}$ for $d \in \{1,2,3\}$.

By using the induction assumption $\|\nabla \boldsymbol{e}_{n-1}\|_{L^2} \le C\tau^{\frac54}$ in (3.9), and the Sobolev embedding $H^2 \hookrightarrow L^4$, the inequality above can be replaced by

$$
\max_{2\le n\le k} \|\boldsymbol{e}_n\|_{L^2}^2 + \tau \sum_{n=2}^{k} \|\nabla \boldsymbol{e}_n\|_{L^2}^2 \le C\tau^4 + C\tau^{\frac14} \sum_{n=1}^{k} \tau^2 (\|\boldsymbol{e}_{n-1}\|_{H^2}^2 + \|\boldsymbol{e}_n\|_{H^2}^2). \quad (3.14)
$$

This requires us to derive a discrete $L^2(0,T;H^2)$ estimate for $\boldsymbol{e}_n$. Besides, we also need to derive an H^3 estimate for $\boldsymbol{e}_k$ to complete the mathematical induction on $\|\boldsymbol{e}_n\|_{H^3} \le \tau^{\frac14}$ in (3.9).

To this end, we shall write the error equation (3.7) into the form of (1.11), with $Q_n = B(\nabla I_\tau \boldsymbol{u}(t_n), \nabla I_\tau \boldsymbol{u}(t_n))$, as shown in (3.28)–(3.29). In Lemma 3.1, we shall prove that the solution of (1.11) satisfies the following discrete $L^2(0,T;H^{s+1})$ estimate:

$$
\max_{2\le n\le k} \sum_{n=2}^{k} \|\boldsymbol{e}_n\|_{H^{s+1}}^2 \le C\sum_{n=2}^{k} \|\boldsymbol{f}_n\|_{H^{s-1}}^2 + C(\|\boldsymbol{e}_0\|_{H^{s+1}}^2 + \|\boldsymbol{e}_1\|_{H^{s+1}}^2), \quad s = 1,2. \quad (3.15)
$$

This estimate will be combined with (3.14) to derive error estimates in L^2, H^1, H^2 and H^3, completing the mathematical induction on (3.9).

3.4. Testing error equation by $\gamma \boldsymbol{e}_n$. Testing equation (3.7) by $\gamma \boldsymbol{e}_n$ (with an artificial parameter γ) and using (3.1a), we obtain

$$
\begin{aligned}
&\int_\Omega \kappa(\nabla I_\tau \boldsymbol{u}_n) \frac{\gamma}{4\tau} |\boldsymbol{e}_n - I_\tau \boldsymbol{e}_n|^2 \mathrm{d}x + \int_\Omega \kappa(\nabla I_\tau \boldsymbol{u}_n)\Big(\frac{\gamma P(\boldsymbol{e}_n)}{4\tau} - \frac{\gamma P(\boldsymbol{e}_{n-1})}{4\tau}\Big)\mathrm{d}x \\
&= -\big((\kappa(\nabla I_\tau \boldsymbol{u}(t_n)) - \kappa(\nabla I_\tau \boldsymbol{u}_n))\delta_\tau \boldsymbol{u}(t_n), \gamma \boldsymbol{e}_n\big)
\end{aligned}
$$

$$
\begin{aligned}
&- (A(\nabla I_\tau \boldsymbol{u}(t_n)) - A(\nabla I_\tau \boldsymbol{u}_n), \gamma \nabla \boldsymbol{e}_n) \\
&- \frac{1}{\alpha}(\nabla(\boldsymbol{e}_n - I_\tau \boldsymbol{e}_n), \gamma \nabla \boldsymbol{e}_n) \\
&+ (\boldsymbol{b}_n + \boldsymbol{d}_n, \gamma \boldsymbol{e}_n) \\
= {}& I_0 + I_1 + I_2 + I_3. \qquad (3.16)
\end{aligned}
$$

Note that

$$
\begin{aligned}
A(\nabla I_\tau \boldsymbol{u}(t_n)) - A(\nabla I_\tau \boldsymbol{u}_n) &= A(\nabla I_\tau \boldsymbol{u}(t_n)) - A(\nabla \boldsymbol{u}(t_n)) \\
&\quad + A(\nabla \boldsymbol{u}(t_n)) - A(\nabla \boldsymbol{u}_n) \\
&\quad + A(\nabla \boldsymbol{u}_n) - A(\nabla I_\tau \boldsymbol{u}_n) \\
&=: I_{11} + I_{12} + I_{13}. \qquad (3.17)
\end{aligned}
$$

By using the notation (3.8), properties (P1)–(P2) and (3.11) imply the following estimates for $2 \le n \le k$:

$$
|I_0| \le K \|\partial_t \boldsymbol{u}\|_{C([0,T];L^\infty)} \|\nabla I_\tau \boldsymbol{e}_n\|_{L^2} \|\boldsymbol{e}_n\|_{L^2}, \qquad (3.18a)
$$

$$
\|I_{11}\| \le K \|\nabla I_\tau \boldsymbol{u}(t_n) - \nabla \boldsymbol{u}(t_n)\|_{L^2} \le C\tau^2, \qquad (3.18b)
$$

$$
(I_{12}, \gamma \nabla \boldsymbol{e}_n) \ge a\gamma \|\nabla \boldsymbol{e}_n\|_{L^2}^2, \qquad (3.18c)
$$

$$
\|I_{13}\| \le K \|\nabla \boldsymbol{u}_n - \nabla I_\tau \boldsymbol{u}_n\|_{L^2} \le K \|\nabla \boldsymbol{e}_n - \nabla I_\tau \boldsymbol{e}_n\|_{L^2} + C\tau^2. \qquad (3.18d)
$$

These estimates imply that

$$
\begin{aligned}
I_1 &= (I_{11} + I_{12} + I_{13}, \gamma \nabla \boldsymbol{e}) \\
&\ge a\gamma \|\nabla \boldsymbol{e}_n\|_{L^2}^2 - \left(C\tau^2 + K\|\nabla \boldsymbol{e}_n - \nabla I_\tau \boldsymbol{e}_n\|\right) \gamma \|\nabla \boldsymbol{e}_n\|_{L^2} \\
&\ge a\gamma \|\nabla \boldsymbol{e}_n\|_{L^2}^2 - C r_1^{-1} \tau^4 - \frac{K^2}{4q_1} \|\nabla \boldsymbol{e}_n - \nabla I_\tau \boldsymbol{e}_n\|_{L^2}^2 - (r_1 + q_1)\gamma^2 \|\nabla \boldsymbol{e}_n\|_{L^2}^2,
\end{aligned}
$$

where r_1 and q_1 are arbitrary positive numbers. Meanwhile, (3.1c) implies that

$$
I_2 \ge \frac{\gamma}{2\alpha}\left(\int_\Omega Q(\nabla \boldsymbol{e}_n)\mathrm{d}x + \|\nabla \boldsymbol{e}_n\|^2 - \|\nabla \boldsymbol{e}_{n-1}\|^2\right) - \frac{\gamma}{\alpha}\left(\int_\Omega \frac{Q(\nabla \boldsymbol{e}_{n-1})}{\ell}\mathrm{d}x + \frac{\ell}{4}\|\nabla \boldsymbol{e}_n\|_{L^2}^2\right).
$$

The truncation error estimate (3.6) implies

$$
I_3 = |(\boldsymbol{b}_n + \boldsymbol{d}_n, \gamma \boldsymbol{e}_n)| \le C r_1^{-1} \tau^4 + r_1 \gamma^2 \|\nabla \boldsymbol{e}_n\|_{L^2}^2.
$$

By substituting the above estimates of I_0, I_1, I_2, I_3 into (3.16), we obtain

$$
\begin{aligned}
&\int_\Omega \kappa(\nabla I_\tau \boldsymbol{u}_n)\frac{\gamma}{4\tau}|\boldsymbol{e}_n - I_\tau \boldsymbol{e}_n|^2 \mathrm{d}x + \int_\Omega \left(\kappa(\nabla I_\tau \boldsymbol{u}_n)\frac{\gamma P(\boldsymbol{e}_n)}{4\tau} - \kappa(\nabla I_\tau \boldsymbol{u}_{n-1})\frac{\gamma P(\boldsymbol{e}_{n-1})}{4\tau}\right)\mathrm{d}x \\
&\quad + \left(a\gamma - (2r_1 + q_1)\gamma^2 - \frac{\ell\gamma}{4\alpha}\right)\|\nabla \boldsymbol{e}_n\|_{L^2}^2 + \left(\frac{\gamma}{2\alpha} - \frac{\gamma}{\ell\alpha}\right)\int_\Omega Q(\nabla \boldsymbol{e}_n)\mathrm{d}x \\
&\quad + \left(\frac{\gamma}{\ell\alpha}\int_\Omega Q(\nabla \boldsymbol{e}_n)\mathrm{d}x + \frac{\gamma}{2\alpha}\|\nabla \boldsymbol{e}_n\|_{L^2}^2 - \frac{\gamma}{\ell\alpha}\int_\Omega Q(\nabla \boldsymbol{e}_{n-1})\mathrm{d}x - \frac{\gamma}{2\alpha}\|\nabla \boldsymbol{e}_{n-1}\|_{L^2}^2\right) \\
&\le C r_1^{-1}\tau^4 + \frac{K^2}{4q_1}\|\nabla \boldsymbol{e}_n - \nabla I_\tau \boldsymbol{e}_n\|_{L^2}^2 \qquad (3.19) \\
&\quad + C\gamma \|\nabla I_\tau \boldsymbol{e}_n\|_{L^2}\|\boldsymbol{e}_n\|_{L^2} + \left(\kappa(\nabla I_\tau \boldsymbol{u}_n) - \kappa(\nabla I_\tau \boldsymbol{u}_{n-1}), \frac{\gamma P(\boldsymbol{e}_{n-1})}{4\tau}\right)
\end{aligned}
$$

$$\le Cr_1^{-1}\tau^4 + \frac{K^2}{4q_1}\|\nabla \boldsymbol{e}_n - \nabla I_\tau \boldsymbol{e}_n\|_{L^2}^2 + C\gamma\|\nabla I_\tau \boldsymbol{e}_n\|_{L^2}\|\boldsymbol{e}_n\|_{L^2}$$
$$+ C\tau^{-1}\|I_\tau(\boldsymbol{u}_n - \boldsymbol{u}_{n-1})\|_{W^{1,\infty}}\|\kappa(\nabla I_\tau \boldsymbol{u}_{n-1})^{-1}\|_{L^\infty}\int_\Omega \kappa(\nabla I_\tau \boldsymbol{u}_{n-1})\frac{\gamma P(\boldsymbol{e}_{n-1})}{4}\mathrm{d}x. \tag{3.20}$$

3.5. Testing error equation by $\boldsymbol{e}_n - \boldsymbol{e}_{n-1}$. Testing (3.7) by $\boldsymbol{e}_n - \boldsymbol{e}_{n-1}$ and using (3.1b), we obtain

$$\begin{aligned}
&\int_\Omega \kappa(\nabla I_\tau \boldsymbol{u}_n)\frac{Q(\boldsymbol{e}_n)}{\tau}\mathrm{d}x + \int_\Omega \kappa(\nabla I_\tau \boldsymbol{u}_n)\Big(\frac{Q(\boldsymbol{e}_n)}{4\tau} - \frac{Q(\boldsymbol{e}_{n-1})}{4\tau}\Big)\mathrm{d}x\\
&\le -\big((\kappa(\nabla I_\tau \boldsymbol{u}(t_n)) - \kappa(\nabla I_\tau \boldsymbol{u}_n))\delta_\tau \boldsymbol{u}(t_n), \boldsymbol{e}_n - \boldsymbol{e}_{n-1}\big)\\
&\quad - (A(\nabla I_\tau \boldsymbol{u}(t_n)) - A(\nabla I_\tau \boldsymbol{u}_n), \nabla(\boldsymbol{e}_n - \boldsymbol{e}_{n-1}))\\
&\quad - \frac{1}{\alpha}(\nabla(\boldsymbol{e}_n - I_\tau \boldsymbol{e}_n), \nabla(\boldsymbol{e}_n - \boldsymbol{e}_{n-1}))\\
&\quad + (\boldsymbol{b}_n + \boldsymbol{d}_n, \boldsymbol{e}_n - \boldsymbol{e}_{n-1})\\
&=: I_4 + I_5 + I_6 + I_7.
\end{aligned} \tag{3.21}$$

Recall that $A(\nabla I_\tau \boldsymbol{u}(t_n)) - A(\nabla I_\tau \boldsymbol{u}_n) = I_{11} + I_{12} + I_{13}$ is defined in (3.17). The estimates (3.18b) and (3.18d) imply

$$(I_{11} + I_{13}, \nabla \boldsymbol{e}_n - \nabla \boldsymbol{e}_{n-1}) \ge -Cp_2^{-1}\tau^4 - \frac{K^2}{4q_2}\|\nabla \boldsymbol{e}_n - \nabla I_\tau \boldsymbol{e}_n\|_{L^2}^2 - (p_2 + q_2)\int_\Omega Q(\nabla \boldsymbol{e}_n)\mathrm{d}x.$$

For the convenience of notation, we denote

$$B_n = B(\nabla \boldsymbol{u}(t_n), \nabla \boldsymbol{u}_n),$$

where the $B(\nabla \boldsymbol{u}(t_n), \nabla \boldsymbol{u}_n)$ is the tensor defined in (2.2). Then

$$\begin{aligned}
&(I_{12}, \nabla \boldsymbol{e}_n - \nabla \boldsymbol{e}_{n-1})\\
&= (B_n \nabla \boldsymbol{e}_n, \nabla \boldsymbol{e}_n) - (B_n \nabla \boldsymbol{e}_n, \nabla \boldsymbol{e}_{n-1})\\
&= \frac{1}{2}(B_n \nabla \boldsymbol{e}_n, \nabla \boldsymbol{e}_n) - \frac{1}{2}(B_n \nabla \boldsymbol{e}_{n-1}, \nabla \boldsymbol{e}_{n-1}) + \frac{1}{2}(B_n \nabla(\boldsymbol{e}_n - \boldsymbol{e}_{n-1}), \nabla(\boldsymbol{e}_n - \boldsymbol{e}_{n-1}))\\
&= \frac{1}{2}(B_n \nabla \boldsymbol{e}_n, \nabla \boldsymbol{e}_n) - \frac{1}{2}(B_{n-1} \nabla \boldsymbol{e}_{n-1}, \nabla \boldsymbol{e}_{n-1}) + \frac{1}{2}(B_n \nabla(\boldsymbol{e}_n - \boldsymbol{e}_{n-1}), \nabla(\boldsymbol{e}_n - \boldsymbol{e}_{n-1})) - J_n\\
&\ge \frac{1}{2}(B_n \nabla \boldsymbol{e}_n, \nabla \boldsymbol{e}_n) - \frac{1}{2}(B_{n-1} \nabla \boldsymbol{e}_{n-1}, \nabla \boldsymbol{e}_{n-1}) + \frac{a}{2}\int_\Omega Q(\nabla \boldsymbol{e}_n)\mathrm{d}x - J_n\,,
\end{aligned}$$

with

$$\begin{aligned}
J_n &= \frac{1}{2}((B_n - B_{n-1})\nabla \boldsymbol{e}_{n-1}, \nabla \boldsymbol{e}_{n-1})\\
&\le C_1\int_\Omega \big(|\nabla(\boldsymbol{u}(t_n) - \boldsymbol{u}(t_{n-1}))| + |\nabla(\boldsymbol{u}_n - \boldsymbol{u}_{n-1})|\big)|\nabla \boldsymbol{e}_{n-1}|^2\mathrm{d}x\\
&\le C_1\int_\Omega \big(|\nabla(\boldsymbol{u}(t_n) - \boldsymbol{u}(t_{n-1}))| + |\nabla(\boldsymbol{e}_n - \boldsymbol{e}_{n-1})|\big)|\nabla \boldsymbol{e}_{n-1}|^2\mathrm{d}x\\
&\le C_1\|\nabla(\boldsymbol{u}(t_n) - \boldsymbol{u}(t_{n-1}))\|_{L^\infty}\|\nabla \boldsymbol{e}_{n-1}\|_{L^2}^2 + C_1\|\nabla(\boldsymbol{e}_n - \boldsymbol{e}_{n-1})\|_{L^4}\|\nabla \boldsymbol{e}_{n-1}\|_{L^4}\|\nabla \boldsymbol{e}_{n-1}\|_{L^2}\\
&\le C_2\tau\|\nabla \boldsymbol{e}_{n-1}\|_{L^2}^2 + C_1\|\nabla \boldsymbol{e}_{n-1}\|_{L^2}(\|\nabla \boldsymbol{e}_{n-1}\|_{L^4}^2 + \|\nabla \boldsymbol{e}_n\|_{L^4}^2),
\end{aligned}$$

where the constant C_1 depends on ϕ, $\|\nabla \boldsymbol{u}(t_n)\|_{L^\infty}$, $\|\nabla \boldsymbol{u}(t_{n-1})\|_{L^\infty}$, $\|\nabla \boldsymbol{u}_n\|_{L^\infty}$ and $\|\nabla \boldsymbol{u}_{n-1}\|_{L^\infty}$. In particular, induction assumption (3.9) implies that $C_1 = \phi(r)/2$. Furthermore, $C_2 = C_1 \|\partial_t u(t)\|_{C([0,T];W^{1,\infty}(\Omega))}$.

Combining the three estimates above, we obtain

$$\begin{aligned}
I_5 \geq\; & \frac{1}{2}(B_n \nabla \boldsymbol{e}_n, \nabla \boldsymbol{e}_n) - \frac{1}{2}(B_{n-1}\nabla \boldsymbol{e}_{n-1}, \nabla \boldsymbol{e}_{n-1}) + \frac{a}{2}\int_\Omega Q(\nabla \boldsymbol{e}_n)\mathrm{d}x - C_2\tau \|\nabla \boldsymbol{e}_{n-1}\|_{L^2}^2 \\
& - C_1 \|\nabla \boldsymbol{e}_{n-1}\|_{L^2}(\|\nabla \boldsymbol{e}_{n-1}\|_{L^4}^2 + \|\nabla \boldsymbol{e}_n\|_{L^4}^2) \\
& - C p_2^{-1}\tau^4 - \frac{K^2}{4q_2}\|\nabla \boldsymbol{e}_n - \nabla I_\tau \boldsymbol{e}_n\|^2 - (p_2 + q_2)\int_\Omega Q(\nabla \boldsymbol{e}_n)\mathrm{d}x.
\end{aligned}$$

Meanwhile, properties (P1) and (3.11) imply

$$\begin{aligned}
|I_4| &\leq K \|\partial_t \boldsymbol{u}\|_{C([0,T];L^\infty)} \|\nabla I_\tau \boldsymbol{e}_n\|_{L^2} \|\boldsymbol{e}_n - \boldsymbol{e}_{n-1}\|_{L^2} \\
&\leq \frac{a\gamma}{24}\|\nabla I_\tau \boldsymbol{e}_n\|_{L^2}^2 + C\gamma^{-1}\|\boldsymbol{e}_n - \boldsymbol{e}_{n-1}\|_{L^2}^2 \\
&\leq \frac{a\gamma}{12}\|\nabla \boldsymbol{e}_{n-1}\|_{L^2}^2 + \frac{a\gamma}{24}\|\nabla \boldsymbol{e}_{n-2}\|_{L^2}^2 + C\gamma^{-1}\|\boldsymbol{e}_n - \boldsymbol{e}_{n-1}\|_{L^2}^2, \qquad (3.23)
\end{aligned}$$

(3.1d) implies

$$I_6 = \frac{1}{2\alpha}\|\nabla(\boldsymbol{e}_n - I_\tau \boldsymbol{e}_n)\|_{L^2}^2 + \int_\Omega \left(\frac{Q(\nabla \boldsymbol{e}_n)}{2\alpha} - \frac{Q(\nabla \boldsymbol{e}_{n-1})}{2\alpha}\right)\mathrm{d}x,$$

and the truncation error estimate (3.6) implies

$$I_7 = |(\boldsymbol{b}_n + \boldsymbol{d}_n, \boldsymbol{e}_n - \boldsymbol{e}_{n-1})| \leq C r_2^{-1}\tau^4 + r_2\|\nabla(\boldsymbol{e}_n - \boldsymbol{e}_{n-1})\|_{L^2}^2$$

for arbitrary number $r_2 > 0$.

By substituting the above estimates of I_4, I_5, I_6, I_7 into (3.21) and using the notation $Q(\boldsymbol{e}_n) = \|\boldsymbol{e}_n - \boldsymbol{e}_{n-1}\|_{L^2}^2$, we obtain

$$\begin{aligned}
& \int_\Omega \kappa(\nabla I_\tau \boldsymbol{u}_n)\frac{Q(\boldsymbol{e}_n)}{\tau}\mathrm{d}x + \int_\Omega \left(\kappa(\nabla I_\tau \boldsymbol{u}_n)\frac{Q(\boldsymbol{e}_n)}{4\tau} - \kappa(\nabla I_\tau \boldsymbol{u}_{n-1})\frac{Q(\boldsymbol{e}_{n-1})}{4\tau}\right)\mathrm{d}x \\
& \quad + \frac{1}{2}(B_n\nabla \boldsymbol{e}_n, \nabla \boldsymbol{e}_n) - \frac{1}{2}(B_{n-1}\nabla \boldsymbol{e}_{n-1}, \nabla \boldsymbol{e}_{n-1}) \\
& \quad + \int_\Omega \frac{a}{2}Q(\nabla \boldsymbol{e}_n)\mathrm{d}x + \frac{1}{2\alpha}\|\nabla(\boldsymbol{e}_n - I_\tau \boldsymbol{e}_n)\|_{L^2}^2 + \int_\Omega \left(\frac{Q(\nabla \boldsymbol{e}_n)}{2\alpha} - \frac{Q(\nabla \boldsymbol{e}_{n-1})}{2\alpha}\right)\mathrm{d}x \\
& \leq C p_2^{-1}\tau^4 + \frac{K^2}{4q_2}\|\nabla \boldsymbol{e}_n - \nabla I_\tau \boldsymbol{e}_n\|_{L^2}^2 + (p_2 + q_2)\int_\Omega Q(\nabla \boldsymbol{e}_n)\mathrm{d}x \qquad (3.24) \\
& \quad + C r_2^{-1}\tau^4 + \int_\Omega r_2 Q(\boldsymbol{e}_n)\mathrm{d}x + C_2\tau\|\nabla \boldsymbol{e}_{n-1}\|_{L^2}^2 \\
& \quad + C_1\|\nabla \boldsymbol{e}_{n-1}\|_{L^2}(\|\nabla \boldsymbol{e}_{n-1}\|_{L^4}^2 + \|\nabla \boldsymbol{e}_n\|_{L^4}^2). \\
& \quad + \frac{a\gamma}{12}\|\nabla \boldsymbol{e}_{n-1}\|_{L^2}^2 + \frac{a\gamma}{24}\|\nabla \boldsymbol{e}_{n-2}\|_{L^2}^2 + C\gamma^{-1}\|\boldsymbol{e}_n - \boldsymbol{e}_{n-1}\|_{L^2}^2 \\
& \quad + C\tau^{-1}\|I_\tau(\boldsymbol{u}_n - \boldsymbol{u}_{n-1})\|_{W^{1,\infty}}\|\kappa(\nabla I_\tau \boldsymbol{u}_{n-1})^{-1}\|_{L^\infty}\int_\Omega \kappa(\nabla I_\tau \boldsymbol{u}_{n-1})\frac{Q(\boldsymbol{e}_{n-1})}{4}\mathrm{d}x,
\end{aligned}$$

where the last term arises similarly as the last term of (3.19).

3.6. Error estimation based on the induction assumption (3.9). Summing up (3.19) and (3.24), we obtain

$$\begin{aligned}
&\frac{E_n - E_{n-1}}{\tau} + \int_\Omega \kappa(\nabla I_\tau \boldsymbol{u}_n)\frac{\gamma}{4\tau}|\boldsymbol{e}_n - I_\tau \boldsymbol{e}_n|^2 \mathrm{d}x \\
&\quad + \left(a\gamma - (r_1 + q_1 + r_1)\gamma^2 - \frac{\ell\gamma}{4\alpha} - \frac{a\gamma}{8}\right)\|\nabla \boldsymbol{e}_n\|_{L^2}^2 \\
&\quad + \left(\frac{a\gamma}{8}\|\nabla \boldsymbol{e}_n\|_{L^2}^2 - \frac{a\gamma}{12}\|\nabla \boldsymbol{e}_{n-1}\|_{L^2}^2 - \frac{a\gamma}{24}\|\nabla \boldsymbol{e}_{n-2}\|_{L^2}^2\right) \\
&\quad + \left(\frac{a}{2} + \frac{\gamma}{2\alpha} - p_2 - q_2 - \frac{\gamma}{\alpha\ell}\right)\int_\Omega Q(\nabla \boldsymbol{e}_n)\mathrm{d}x + \int_\Omega \left(\frac{1}{\tau}\kappa(\nabla I_\tau \boldsymbol{u}_n) - r_2\right)Q(\boldsymbol{e}_n)\mathrm{d}x
\end{aligned} \tag{3.25}$$

$$\begin{aligned}
&\quad + \left(\frac{1}{2\alpha} - \frac{K^2}{4q_1} - \frac{K^2}{4q_2}\right)\|\nabla(\boldsymbol{e}_n - I_\tau \boldsymbol{e}_n)\|_{L^2}^2 \\
&\le C\big(r_1^{-1} + p_2^{-1} + r_2^{-1}\big)\tau^4 + C\|\nabla \boldsymbol{e}_{n-1}\|_{L^2}(\|\nabla \boldsymbol{e}_{n-1}\|_{L^4}^2 + \|\nabla \boldsymbol{e}_n\|_{L^4}^2), \\
&\quad + C(1 + \gamma^{-1} + \tau^{-1}\|I_\tau(\boldsymbol{u}_n - \boldsymbol{u}_{n-1})\|_{W^{1,\infty}})E_{n-1}
\end{aligned} \tag{3.26}$$

with

$$\begin{aligned}
E_n = &\int_\Omega \left(\kappa(\nabla I_\tau \boldsymbol{u}_n)\frac{\gamma}{4}P(\boldsymbol{e}_n) + \kappa(\nabla I_\tau \boldsymbol{u}_n)\frac{Q(\boldsymbol{e}_n)}{4}\right)\mathrm{d}x \\
&+ \tau\left[\frac{\gamma}{2\alpha}\|\nabla \boldsymbol{e}_n\|_{L^2}^2 + \int_\Omega \left(\frac{1}{2\alpha} + \frac{\gamma}{\alpha\ell}\right)Q(\nabla \boldsymbol{e}_n)\mathrm{d}x + \frac{1}{2}(B_n\nabla \boldsymbol{e}_n, \nabla \boldsymbol{e}_n)\right].
\end{aligned}$$

For any given parameter $\alpha \le \dfrac{a}{2K^2}$, we can choose

$$q_1 = \frac{a}{8\gamma}, \quad q_2 = \frac{a}{4}, \quad r_1 = 1, \quad r_2 = \frac{1}{2\tau\phi(r)}, \quad p_2 = \frac{a}{8}, \quad \ell = \frac{a\alpha}{2}$$

and a sufficiently small number γ (independently of τ), to make the following inequalities hold:

$$\begin{aligned}
&a\gamma - (r_1 + q_1 + r_1)\gamma^2 - \frac{\ell\gamma}{4\alpha} \ge \frac{a\gamma}{4}, \\
&\frac{a}{2} + \frac{\gamma}{2\alpha} - p_2 - q_2 - \frac{\gamma}{\alpha\ell} \ge 0, \\
&\frac{1}{2\alpha} - \frac{K^2}{4q_1} - \frac{K^2}{4q_2} \ge 0.
\end{aligned}$$

Therefore, substituting the above inequalities into (3.25), we obtain for $n = 2, \ldots, k$ (such that the induction assumption (3.9) holds)

$$\begin{aligned}
&\frac{E_n - E_{n-1}}{\tau} + \frac{a\gamma}{4}\|\nabla \boldsymbol{e}_n\|_{L^2}^2 + \int_\Omega \frac{\kappa(\nabla I_\tau \boldsymbol{u}_n)}{2\tau}Q(\boldsymbol{e}_n)\mathrm{d}x \\
&\le C\tau^4 + C\|\nabla \boldsymbol{e}_{n-1}\|_{L^2}(\|\nabla \boldsymbol{e}_{n-1}\|_{L^4}^2 + \|\nabla \boldsymbol{e}_n\|_{L^4}^2) \\
&\quad + C(1 + \tau^{-1}\|I_\tau(\boldsymbol{u}_n - \boldsymbol{u}_{n-1})\|_{W^{1,\infty}})E_{n-1}.
\end{aligned}$$

By using Gronwall's inequality (cf. [12]), we obtain

$$\max_{2\le n\le k} E_n + \sum_{n=1}^{k}\left(\frac{a\gamma}{4}\tau\|\nabla \boldsymbol{e}_n\|_{L^2}^2 + \int_\Omega \frac{\kappa(\nabla I_\tau \boldsymbol{u}_n)}{2}Q(\boldsymbol{e}_n)\mathrm{d}x\right)$$

$$\leq C_g\left(E_1 + C\tau^4 + C_3\sum_{n=1}^{k}\tau\|\nabla \boldsymbol{e}_{n-1}\|_{L^2}(\|\nabla \boldsymbol{e}_{n-1}\|_{L^4}^2 + \|\nabla \boldsymbol{e}_n\|_{L^4}^2)\right)$$

$$\leq C\tau^4 + C_3\sum_{n=1}^{k}\tau\|\nabla \boldsymbol{e}_{n-1}\|_{L^2}(\|\nabla \boldsymbol{e}_{n-1}\|_{L^4}^2 + \|\nabla \boldsymbol{e}_n\|_{L^4}^2), \tag{3.27}$$

where

$$C_g = \exp\left(C\sum_{n=2}^{k}(\tau + \|I_\tau(\boldsymbol{u}_n - \boldsymbol{u}_{n-1})\|_{W^{1,\infty}})\right) \leq \exp(CC_*),$$

we have used (3.12) and (A1) in deriving the last inequality of (3.27). This gives us a constant C_3 independent of k.

By using the tensor $B(\nabla \boldsymbol{u}, \nabla \boldsymbol{v})$ defined in (2.2), we can rewrite (3.7) as

$$\begin{aligned}
&\nabla\cdot[B(\nabla I_\tau \boldsymbol{u}(t_n), \nabla I_\tau \boldsymbol{u}(t_n))\nabla \boldsymbol{e}_n] + \frac{1}{\alpha}(\Delta \boldsymbol{e}_n - \Delta I_\tau \boldsymbol{e}_n)\\
&= \boldsymbol{f}_n + \nabla\cdot[(B(\nabla I_\tau \boldsymbol{u}(t_n), \nabla I_\tau \boldsymbol{u}(t_n)) - B(\nabla I_\tau \boldsymbol{u}(t_n), \nabla I_\tau \boldsymbol{u}_n))\nabla \boldsymbol{e}_n]
\end{aligned} \tag{3.28}$$

with

$$\boldsymbol{f}_n = \kappa(\nabla I_\tau \boldsymbol{u}_n)\,\delta_\tau \boldsymbol{e}_n + (\kappa(\nabla I_\tau \boldsymbol{u}(t_n)) - \kappa(\nabla I_\tau \boldsymbol{u}_n))\delta_\tau \boldsymbol{u}(t_n) - \boldsymbol{b}_n - \boldsymbol{d}_n. \tag{3.29}$$

Since $Q(\boldsymbol{e}_n) = |\boldsymbol{e}_n - \boldsymbol{e}_{n-1}|^2$, we have from (3.27)

$$\begin{aligned}
\sum_{n=1}^{k}\tau^2\left\|\frac{\boldsymbol{e}_n - \boldsymbol{e}_{n-1}}{\tau}\right\|_{L^2}^2 &= \sum_{n=1}^{k}\int_\Omega Q(\boldsymbol{e}_n)\mathrm{d}x\\
&\leq C\tau^4 + 2C_3\sum_{n=1}^{k}\tau\|\nabla \boldsymbol{e}_{n-1}\|_{L^2}(\|\nabla \boldsymbol{e}_{n-1}\|_{L^4}^2 + \|\nabla \boldsymbol{e}_n\|_{L^4}^2).
\end{aligned} \tag{3.30}$$

Hence, the function $\boldsymbol{f}_n$ satisfies

$$\begin{aligned}
\sum_{n=2}^{k}\tau^2\|\boldsymbol{f}_n\|_{L^2}^2 &\leq C\sum_{n=2}^{k}\tau^2\left\|\frac{1}{\tau}\left(\frac{3}{2}\boldsymbol{e}_n - 2e_{n-1} + \frac{1}{2}e_{n-2}\right)\right\|_{L^2}^2\\
&\quad + C\sum_{n=2}^{k}\tau^2\|\nabla I_\tau \boldsymbol{e}_n\|_{L^2}^2 + \sum_{n=2}^{k}\tau^2\|\boldsymbol{b}_n + \boldsymbol{d}_n\|_{L^2}^2\\
&\leq C\sum_{n=1}^{k}\tau^2\left\|\frac{\boldsymbol{e}_n - \boldsymbol{e}_{n-1}}{\tau}\right\|_{L^2}^2 + C\sum_{n=2}^{k}\tau^2\|\nabla I_\tau \boldsymbol{e}_n\|_{L^2}^2 + C\tau^4\\
&\leq C\tau^4 + 5C_3\sum_{n=1}^{k}\tau\|\nabla \boldsymbol{e}_{n-1}\|_{L^2}(\|\nabla \boldsymbol{e}_{n-1}\|_{L^4}^2 + \|\nabla \boldsymbol{e}_n\|_{L^4}^2),
\end{aligned} \tag{3.31}$$

where the last inequality uses (3.30) and (3.27). The latter gives us an estimate for the term $\sum_{n=2}^{k}\tau^2\|\nabla I_\tau \boldsymbol{e}_n\|_{L^2}^2$.

To estimate the right-hand side of (3.31), we need the following lemma, which will be proved in Section 4.

Lemma 3.1. *Let $s \in \{0,1,2\}$ and $\beta \in (0,1]$ be fixed. Let $Q_n \in W^{s,\infty}(\Omega)^{d\times m\times d\times m}$, $n = 2,\dots,k$, be a sequence of tensor-valued functions such that*

$$Q_n\xi \cdot \xi \ge a|\xi|^2 \quad \text{and} \quad |Q_n\xi| \le K|\xi|, \quad \forall\, \xi \in \mathbb{R}^{d\times m},$$

and

$$\|Q_n\|_{W^{s,\infty}} \le C_0, \qquad 2 \le n \le k, \tag{3.32}$$

$$\|Q_n - Q_l\|_{H^2} \le C_0|t_l - t_n|^{\beta}, \qquad 2 \le n \le l \le k. \tag{3.33}$$

If $\boldsymbol{e}_n \in H_0^1(\Omega)$ is the weak solution of

$$\nabla \cdot Q_n \nabla \boldsymbol{e}_n + \frac{1}{\alpha}(\Delta \boldsymbol{e}_n - \Delta I_\tau \boldsymbol{e}_n) = \boldsymbol{f}_n, \quad n = 2,\dots,k, \tag{3.34}$$

then there exists a positive constant C such that

$$\sum_{n=2}^{k} \|\boldsymbol{e}_n\|_{H^{s+1}}^2 \le C \sum_{n=2}^{k} \|\boldsymbol{f}_n\|_{H^{s-1}}^2 + C(\|\boldsymbol{e}_0\|_{H^{s+1}}^2 + \|\boldsymbol{e}_1\|_{H^{s+1}}^2). \tag{3.35}$$

The constant C may depend on a, K, C_0 and β, but is independent of k.

Let

$$Q_n = B(\nabla I_\tau \boldsymbol{u}(t_n), \nabla I_\tau \boldsymbol{u}(t_n)) \quad \text{and} \quad \hat{Q}_n = B(\nabla I_\tau \boldsymbol{u}(t_n), \nabla I_\tau \boldsymbol{u}_n). \tag{3.36}$$

Then, due to the induction assumption (3.9), we have

$$\|Q_n - \hat{Q}_n\|_{H^2} \le C\|I_\tau \boldsymbol{e}_n\|_{H^3} \le C\tau^{\frac{1}{4}}. \tag{3.37}$$

Since the exact solution $\boldsymbol{u}(t_n)$ is sufficiently smooth, the tensor-valued function Q_n defined in (3.36) satisfies the conditions of Lemma 3.1 for $s = 0,1,2$ with $\beta = 1$. Hence, by applying Lemma 3.1 to (3.28) with $s = 1$, we obtain

$$\begin{aligned}
\sum_{n=2}^{k} \tau^2 \|\boldsymbol{e}_n\|_{H^2}^2 &\le C \sum_{n=2}^{k} \tau^2 \|\boldsymbol{f}_n\|_{L^2}^2 + C\tau^2(\|\boldsymbol{e}_0\|_{H^2}^2 + \|\boldsymbol{e}_1\|_{H^2}^2) \\
&\quad + C \sum_{n=2}^{k} \tau^2 \|\nabla \cdot [(Q_n - \hat{Q}_n)\nabla \boldsymbol{e}_n]\|_{L^2}^2 \\
&\le C \sum_{n=2}^{k} \tau^2 \|\boldsymbol{f}_n\|_{L^2}^2 + C\tau^2(\|\boldsymbol{e}_0\|_{H^2}^2 + \|\boldsymbol{e}_1\|_{H^2}^2) \\
&\quad + C \sum_{n=2}^{k} \tau^2 \|Q_n - \hat{Q}_n\|_{W^{1,3}}^2 \|I_\tau \boldsymbol{e}_n\|_{W^{1,6}}^2 + C \sum_{n=2}^{k} \tau^2 \|Q_n - \hat{Q}_n\|_{L^\infty}^2 \|I_\tau \boldsymbol{e}_n\|_{H^2}^2 \\
&\le C \sum_{n=2}^{k} \tau^2 \|\boldsymbol{f}_n\|_{L^2}^2 + C\tau^2(\|\boldsymbol{e}_0\|_{H^2}^2 + \|\boldsymbol{e}_1\|_{H^2}^2) + C\tau^{\frac{1}{2}} \sum_{n=2}^{k} \tau^2 \|I_\tau \boldsymbol{e}_n\|_{H^2}^2.
\end{aligned} \tag{3.38}$$

Substituting this into (3.31) and using assumption (A4), we have

$$\sum_{n=2}^{k} \tau^2 \|\boldsymbol{e}_n\|_{H^2}^2$$

$$\le C\tau^4 + C\sum_{n=2}^{k}\tau\|\nabla \boldsymbol{e}_{n-1}\|_{L^2}(\|\nabla \boldsymbol{e}_{n-1}\|_{L^4}^2 + \|\nabla \boldsymbol{e}_n\|_{L^4}^2) + C\tau^{\frac12}\sum_{n=2}^{k}\tau^2\|I_\tau \boldsymbol{e}_n\|_{H^2}^2$$
$$\le C\tau^4 + C_4\tau^{\frac14}\sum_{n=2}^{k}\tau^2(\|\boldsymbol{e}_{n-2}\|_{H^2}^2 + \|\boldsymbol{e}_{n-1}\|_{H^2}^2 + \|\boldsymbol{e}_n\|_{H^2}^2), \tag{3.39}$$

with constants C and C_4 independent of k, where we have used the induction assumption $\|\boldsymbol{e}_{n-1}\|_{H^1} \le \tau^{\frac54}$ in (3.9). For sufficiently small stepsize τ satisfying $\tau^{\frac14} \le (4C_4)^{-1}$, the second term on the right-hand side of (3.39) can be absorbed by the left-hand side. Then (3.39) is reduced to

$$\sum_{n=2}^{k}\tau^2\|\boldsymbol{e}_n\|_{H^2}^2 \le C\tau^4. \tag{3.40}$$

Substituting (3.40) into (3.27) and using the induction assumption $\|\boldsymbol{e}_{n-1}\|_{H^1} \le \tau^{\frac54}$, we obtain

$$\max_{2\le n\le k} E_n + \sum_{n=2}^{k}\tau\|\nabla \boldsymbol{e}_n\|_{L^2}^2 \le C\tau^4.$$

In particular, since $\|\boldsymbol{e}_n\|_{L^2}^2 \le CE_n$, it follows that

$$\|\boldsymbol{e}_n\|_{L^2}^2 + \sum_{n=2}^{k}\tau\|\boldsymbol{e}_n\|_{H^1}^2 \le C\tau^4. \tag{3.41}$$

This also implies

$$\sum_{n=2}^{k}\tau\left\|\frac{\boldsymbol{e}_n - \boldsymbol{e}_{n-1}}{\tau}\right\|_{H^1}^2 \le C\tau^2.$$

Hence,

$$\sum_{n=2}^{k}\|\boldsymbol{e}_n - \boldsymbol{e}_{n-1}\|_{H^1} = \sum_{n=2}^{k}\tau\left\|\frac{\boldsymbol{e}_n - \boldsymbol{e}_{n-1}}{\tau}\right\|_{H^1} \le T^{\frac12}\left(\sum_{n=2}^{k}\tau\left\|\frac{\boldsymbol{e}_n - \boldsymbol{e}_{n-1}}{\tau}\right\|_{H^1}^2\right)^{\frac12} \le C\tau. \tag{3.42}$$

3.7. Completing the mathematical induction. The estimate (3.41) further implies

$$\sum_{n=2}^{k}\|\delta_\tau \boldsymbol{e}_n\|_{H^1}^2 \le C\tau. \tag{3.43}$$

By using the expression of $\boldsymbol{f}_n$ in (3.29), we derive that

$$\sum_{n=2}^{k}\|\boldsymbol{f}_n\|_{H^1}^2 \le C\sum_{n=2}^{k}\|\delta_\tau \boldsymbol{e}_n\|_{H^1}^2 + C\sum_{n=2}^{k}\|\boldsymbol{e}_{n-1}\|_{H^2}^2 + C\sum_{n=2}^{k}\|\boldsymbol{b}_n + \boldsymbol{d}_n\|_{H^1}^2 \le C\tau,$$

where we have used (3.43) and (3.40). By applying Lemma 3.1 to the equation (3.28) with $s = 2$, we obtain

$$\begin{aligned}\sum_{n=2}^{k} \|\boldsymbol{e}_n\|_{H^3}^2 &\le C \sum_{n=2}^{k} \|\boldsymbol{f}_n\|_{H^1}^2 + C(\|\boldsymbol{e}_0\|_{H^3}^2 + \|\boldsymbol{e}_1\|_{H^3}^2) \\ &\quad + C \sum_{n=2}^{k} \tau^2 \|\nabla \cdot [(Q_n - \hat{Q}_n)\nabla \boldsymbol{e}_n]\|_{H^1}^2 \\ &\le C\tau + C \sum_{n=2}^{k} \|Q_n - \hat{Q}_n\|_{H^2}^2 \|\boldsymbol{e}_n\|_{W^{1,\infty}}^2 \\ &\quad + C \sum_{n=2}^{k} \|Q_n - \hat{Q}_n\|_{W^{1,3}}^2 \|\boldsymbol{e}_n\|_{W^{2,6}}^2 \\ &\quad + C \sum_{n=2}^{k} \|Q_n - \hat{Q}_n\|_{L^\infty}^2 \|\boldsymbol{e}_n\|_{H^3}^2 \\ &\le C\tau + C\tau^{\frac{1}{2}} \sum_{n=2}^{k} \|\boldsymbol{e}_n\|_{H^3}^2, \end{aligned} \tag{3.44}$$

where we have used assumption (A4) and (3.37) again. For sufficiently small τ the second term on the right-hand side above can be absorbed by the left-hand side. Hence, we have

$$\sum_{n=2}^{k} \|\boldsymbol{e}_n\|_{H^3}^2 \le C\tau, \tag{3.45}$$

which furthermore implies

$$\sum_{n=2}^{k} \tau \left\| \frac{\boldsymbol{e}_n - \boldsymbol{e}_{n-1}}{\tau} \right\|_{H^3}^2 \le C \tag{3.46}$$

and

$$\max_{2 \le n \le k} \|\boldsymbol{e}_n\|_{H^3} \le C\tau^{\frac{1}{2}}. \tag{3.47}$$

The estimate (3.46) implies

$$\sum_{n=2}^{k} \|\boldsymbol{e}_n - \boldsymbol{e}_{n-1}\|_{H^3} = \sum_{n=2}^{k} \tau \left\| \frac{\boldsymbol{e}_n - \boldsymbol{e}_{n-1}}{\tau} \right\|_{H^3} \le T^{\frac{1}{2}} \left(\sum_{n=2}^{k} \tau \left\| \frac{\boldsymbol{e}_n - \boldsymbol{e}_{n-1}}{\tau} \right\|_{H^3}^2 \right)^{\frac{1}{2}} \le C \tag{3.48}$$

and therefore, using the Sobolev interpolation inequality,

$$\begin{aligned}\sum_{n=2}^{k} \|\boldsymbol{e}_n - \boldsymbol{e}_{n-1}\|_{W^{1,\infty}} &\le \sum_{n=2}^{k} \|\boldsymbol{e}_n - \boldsymbol{e}_{n-1}\|_{H^1}^{1-\frac{d}{4}} \|\boldsymbol{e}_n - \boldsymbol{e}_{n-1}\|_{H^3}^{\frac{d}{4}} \\ &\le \left(\sum_{n=2}^{k} \|\boldsymbol{e}_n - \boldsymbol{e}_{n-1}\|_{H^1} \right)^{1-\frac{d}{4}} \left(\sum_{n=2}^{k} \|\boldsymbol{e}_n - \boldsymbol{e}_{n-1}\|_{H^3} \right)^{\frac{d}{4}} \end{aligned}$$

$$\le C\tau^{1-\frac{d}{4}}, \tag{3.49}$$

where we have used (3.42) and (3.48) in the last inequality.

Since $H^3(\Omega) \hookrightarrow W^{1,\infty}(\Omega)$ for $d = 1, 2, 3$, for sufficiently small τ (independent of k) the estimates (3.41) and (3.47)–(3.49) imply (3.9). This completes the mathematical induction. Therefore, the estimates (3.40)–(3.41) and (3.46) hold for all $2 \le k \le N$.

This proves Theorem 2.1 for sufficiently small stepsize $\tau \le \tau_0$, where τ_0 is some positive constant. If $\tau \ge \tau_0$, then the number of time steps is bounded by the constant T/τ_0. In this case, we can regard (1.10) as an elliptic equation (with a stepsize τ being bounded from below by τ_0). If we denote $\Phi_n = \|\boldsymbol{u}_n\|_{H^3}$, then the standard H^3 estimate for (1.10) implies that

$$\Phi_n \le \psi(\Phi_{n-1} + \Phi_{n-2}),$$

where $\psi : \mathbb{R}_+ \to \mathbb{R}_+$ is some increasing function (depending on the constant τ_0). Iterating the inequality above at most T/τ_0 times yields

$$\max_{2\le n\le N} \Phi_n \le C.$$

This proves

$$\max_{2\le n\le N} \|\boldsymbol{u}_n - \boldsymbol{u}(t_n)\|_{H^3} \le \max_{2\le n\le N} \|\boldsymbol{u}_n\|_{H^3} + \max_{2\le n\le N} \|\boldsymbol{u}(t_n)\|_{H^3} \le C \le C\tau_0^{-2}\tau^2,$$

where the last inequality is due to $\tau \ge \tau_0$. Hence, combining the two cases $\tau \le \tau_0$ and $\tau \ge \tau_0$, we obtain the desired error estimate in Theorem 2.1. It remains to prove Lemma 3.1 to complete the proof of Theorem 2.1. This is presented in the next section. □

4. Proof of Lemma 3.1. We need the following result to prove Lemma 3.1. This is the case of Lemma 3.1 with time-independent coefficient $Q_n = Q$ for $n \ge 2$.

Lemma 4.1. *Let $\Omega \subset \mathbb{R}^d$ be a bounded smooth domain. Let $s \in \{0, 1, 2\}$ be fixed and assume that $Q \in W^{s,\infty}(\Omega)^{d\times m\times d\times m}$ is a symmetric real tensor-valued function such that*

$$Q(x)\xi \cdot \xi \ge a|\xi|^2 \quad \textit{and} \quad |Q(x)\xi| \le K|\xi|, \quad \forall\, \xi \in \mathbb{R}^{d\times m}, \quad \forall\, x \in \Omega.$$

If $\boldsymbol{e}_n \in H^1_0(\Omega)$ is a weak solution of

$$\nabla \cdot Q\nabla \boldsymbol{e}_n + \frac{1}{\alpha}(\Delta \boldsymbol{e}_n - \Delta I_\tau \boldsymbol{e}_n) = \boldsymbol{f}_n, \quad n = 2, \dots, k, \tag{4.1}$$

then

$$\sum_{n=2}^{k} \|\boldsymbol{e}_n\|^2_{H^{s+1}} \le C \sum_{n=2}^{k} \|\boldsymbol{f}_n\|^2_{H^{s-1}} + C(\|\boldsymbol{e}_0\|^2_{H^{s+1}} + \|\boldsymbol{e}_1\|^2_{H^{s+1}}), \tag{4.2}$$

where the constant C is independent of k.

Proof. Without loss of generality, we can set $\boldsymbol{f}_n = 0$ for $n \ge k + 1$, and this does not affect the values of $\boldsymbol{e}_n$ for $n = 2, \dots, k$. Then, multiplying (4.1) by ζ^n and summing up the equations for $n = 2, 3, \dots,$ and denoting $\widetilde{\boldsymbol{e}}(\zeta) = \sum_{n=2}^{\infty} \boldsymbol{e}_n\zeta^n$, we obtain

$$\nabla \cdot [(Q + \delta(\zeta)I)\nabla \widetilde{\boldsymbol{e}}(\zeta)] = \widetilde{\boldsymbol{f}}(\zeta) \quad \text{for } \zeta \in \mathbb{C},\ |\zeta| = 1. \tag{4.3}$$

with $\delta(\zeta)=\dfrac{1}{\alpha}(1-\zeta)^2$ and

$$\widetilde{\boldsymbol{f}}(\zeta)=\sum_{n=2}^{\infty}\boldsymbol{f}_n\zeta^n+\frac{\zeta^2}{\alpha}\Delta(2\boldsymbol{e}_1-\boldsymbol{e}_0)-\frac{\zeta^3}{\alpha}\Delta\boldsymbol{e}_1.$$

Since Q is real-valued and symmetric positive definite, it follows that $Q\xi\cdot\xi\in\mathbb{R}$ and $Q\xi\cdot\xi\geq a|\xi|^2$ for $\xi\in\mathbb{C}^d$. Hence, there exists a positive constant κ such that for $|\zeta|=1$ and $|\zeta-1|\leq\kappa$ there holds

$$\mathrm{Re}[(Q+\delta(\zeta)I)\xi\cdot\xi]\geq\frac{a}{2}|\xi|^2. \tag{4.4}$$

For $|\zeta|=1$ and $|\zeta-1|\geq\kappa$, there holds $|\mathrm{Im}(\delta(\zeta))|\geq 1/C$. Without loss of generality, we assume $\mathrm{Im}(\delta(\zeta))\geq 1/C$ for the given ζ and consider the following reformulation:

$$\nabla\cdot[-i(Q+\delta(\zeta)I)\nabla\widetilde{\boldsymbol{e}}(\zeta)]=i\widetilde{\boldsymbol{f}}(\zeta). \tag{4.5}$$

Otherwise $\mathrm{Im}(\delta(\zeta))\leq -1/C$ and we consider

$$\nabla\cdot[i(Q+\delta(\zeta)I)\nabla\widetilde{\boldsymbol{e}}(\zeta)]=-i\widetilde{\boldsymbol{f}}(\zeta). \tag{4.6}$$

In the case $\mathrm{Im}(\delta(\zeta))\geq 1/C$, the coefficients of (4.5) satisfy the ellipticity condition

$$\mathrm{Re}[-i(Q+\delta(\zeta)I)\xi\cdot\xi]=\mathrm{Im}(\delta(\zeta))|\xi|^2\geq C^{-1}|\xi|^2. \tag{4.7}$$

In either case, $|\zeta-1|\leq\kappa$ or $|\zeta-1|\geq\kappa$, (4.3) can be formulated as an elliptic equation with coefficients satisfying the ellipticity condition (4.4) or (4.7) respectively. Hence, the solution of (4.3) satisfies (see Appendix)

$$\|\widetilde{\boldsymbol{e}}(\zeta)\|_{H^{s+1}}\leq C\|\widetilde{\boldsymbol{f}}(\zeta)\|_{H^{s-1}}. \tag{4.8}$$

Then, by using Parseval's identity $\sum_{n=2}^{\infty}\|\boldsymbol{e}_n\|_{H^{s+1}}^2=\frac{1}{2\pi}\int_{|\zeta|=1}\|\widetilde{\boldsymbol{e}}(\zeta)\|_{H^{s+1}}^2|\mathrm{d}\zeta|$, where $|\mathrm{d}\zeta|$ denotes the arg-length element on the unit circle of the complex plane, we obtain

$$\begin{aligned}\sum_{n=2}^{k}\|\boldsymbol{e}_n\|_{H^{s+1}}^2\leq\sum_{n=2}^{\infty}\|\boldsymbol{e}_n\|_{H^{s+1}}^2&=\frac{1}{2\pi}\int_{|\zeta|=1}\|\widetilde{\boldsymbol{e}}(\zeta)\|_{H^{s+1}}^2|\mathrm{d}\zeta|\\&\leq\frac{C}{2\pi}\int_{|\zeta|=1}\|\widetilde{\boldsymbol{f}}(\zeta)\|_{H^{s-1}}^2|\mathrm{d}\zeta|\\&\leq C\sum_{n=2}^{\infty}\|\boldsymbol{f}_n\|_{H^{s-1}}^2+C(\|\Delta\boldsymbol{e}_0\|_{H^{s-1}}^2+\|\Delta\boldsymbol{e}_1\|_{H^{s-1}}^2)\\&\leq C\sum_{n=2}^{k}\|\boldsymbol{f}_n\|_{H^{s-1}}^2+C(\|\boldsymbol{e}_0\|_{H^{s+1}}^2+\|\boldsymbol{e}_1\|_{H^{s+1}}^2).\end{aligned}$$

This proves Lemma 4.1. □

To prove Lemma 3.1, we rewrite equation (3.34) as

$$\nabla\cdot Q_l\nabla\boldsymbol{e}_n+\frac{1}{\alpha}(\Delta\boldsymbol{e}_n-\Delta I_\tau\boldsymbol{e}_n)=\boldsymbol{f}_n+\nabla\cdot[(Q_l-Q_n)\nabla\boldsymbol{e}_n], \tag{4.9}$$

and consider the equation above for $n = 2, \dots, l$. Since Q_l is fixed for $n = 2, \dots, l$, we can apply the result of Lemma 4.1. This yields the following estimate for $s = 0, 1, 2$:

$$\begin{aligned}\sum_{n=2}^{l} \|\boldsymbol{e}_n\|_{H^{s+1}}^2 &\le C \sum_{n=2}^{l} \|\boldsymbol{f}_n + \nabla\cdot[(Q_l - Q_n)\nabla \boldsymbol{e}_n]\|_{H^{s-1}}^2 + C(\|\boldsymbol{e}_0\|_{H^{s+1}}^2 + \|\boldsymbol{e}_1\|_{H^{s+1}}^2) \\ &\le C \sum_{n=2}^{l} (\|\boldsymbol{f}_n\|_{H^{s-1}}^2 + C\|Q_l - Q_n\|_{H^2}^2 \|\boldsymbol{e}_n\|_{H^{s+1}}^2) + C(\|\boldsymbol{e}_0\|_{H^{s+1}}^2 + \|\boldsymbol{e}_1\|_{H^{s+1}}^2) \\ &\le C \sum_{n=2}^{l} \|\boldsymbol{f}_n\|_{H^{s-1}}^2 + C \sum_{n=2}^{l} (t_l - t_n)^{2\beta} \|\boldsymbol{e}_n\|_{H^{s+1}}^2 + C(\|\boldsymbol{e}_0\|_{H^{s+1}}^2 + \|\boldsymbol{e}_1\|_{H^{s+1}}^2).\end{aligned}$$

where the term $\|Q_l - Q_n\|_{H^2}^2 \|\boldsymbol{e}_n\|_{H^{s+1}}^2$ is obtained similarly as (3.44) by combining several norms on $Q_l - Q_n$ and using Sobolev embedding (details are omitted). If we denote $F_l = \sum_{n=2}^{l} \|\boldsymbol{e}_n\|_{H^{s+1}}^2$ for $l \ge 2$ and $F_1 = 0$, then the inequality above can be rewritten as

$$\begin{aligned}F_l &\le C \sum_{n=2}^{l} \|\boldsymbol{f}_n\|_{H^{s-1}}^2 + C(\|\boldsymbol{e}_0\|_{H^{s+1}}^2 + \|\boldsymbol{e}_1\|_{H^{s+1}}^2) + C \sum_{n=2}^{l} (t_l - t_n)^{2\beta} (F_n - F_{n-1}) \\ &= C \sum_{n=2}^{l} \|\boldsymbol{f}_n\|_{H^{s-1}}^2 + C(\|\boldsymbol{e}_0\|_{H^{s+1}}^2 + \|\boldsymbol{e}_1\|_{H^{s+1}}^2) + C \sum_{n=2}^{l-1} [(t_l - t_n)^{2\beta} - (t_l - t_{n+1})^{2\beta}] F_n \\ &\le C \sum_{n=2}^{l} \|\boldsymbol{f}_n\|_{H^{s-1}}^2 + C(\|\boldsymbol{e}_0\|_{H^{s+1}}^2 + \|\boldsymbol{e}_1\|_{H^{s+1}}^2) + C \sum_{n=2}^{l-1} \tau (t_l - t_n)^{2\beta-1} F_n.\end{aligned}$$

By using Gronwall's inequality with weakly singular kernel (cf. [4, Lemma 6]) we obtain

$$F_l \le C \sum_{n=2}^{l} \|\boldsymbol{f}_n\|_{H^{s-1}}^2 + C(\|\boldsymbol{e}_0\|_{H^{s+1}}^2 + \|\boldsymbol{e}_1\|_{H^{s+1}}^2), \quad l = 2, \dots, k.$$

This implies

$$\sum_{n=2}^{k} \|\boldsymbol{e}_n\|_{H^{s+1}}^2 \le C \sum_{n=2}^{k} \|\boldsymbol{f}_n\|_{H^{s-1}}^2 + C(\|\boldsymbol{e}_0\|_{H^{s+1}}^2 + \|\boldsymbol{e}_1\|_{H^{s+1}}^2).$$

This completes the proof of Lemma 3.1. ◻

5. Application to other nonlinear parabolic systems. In this section, we demonstrate that both the numerical method and the convergence analysis in this article are applicable to more general nonlinear parabolic problems, including generalized Newtonian fluid flow and some nonlinear parabolic systems of non-divergence form.

5.1. Generalized Newtonian fluid flow. When the viscosity μ of a fluid is not constant, it is often a nonlinear function $\mu = \mu(|\mathbb{D}(\boldsymbol{u})|)$ of the strain tensor

$$\mathbb{D}(\boldsymbol{u}) = \frac{1}{2}(\nabla \boldsymbol{u} + (\nabla \boldsymbol{u})^\top),$$

where $\boldsymbol{u}$ represents the velocity of fluid; see [14] or [26, Section 12.1]. In this case, the generalized Newtonian fluid flow is described by

$$\begin{aligned} \partial_t \boldsymbol{u} + \boldsymbol{u}\cdot\nabla\boldsymbol{u} - \nabla\cdot A(\nabla\boldsymbol{u}) + \nabla p = 0 & \quad \text{in } \Omega\times(0,T], \\ \nabla\cdot\boldsymbol{u} = 0 & \quad \text{in } \Omega\times(0,T], \\ \boldsymbol{u} = 0 & \quad \text{on } \partial\Omega\times(0,T], \\ \boldsymbol{u}|_{t=0} = \boldsymbol{u}_0 & \quad \text{in } \Omega. \end{aligned} \tag{5.1}$$

with

$$A(\xi)_{ij} = \frac{\partial}{\partial \xi_{ij}} F(|\mathbb{D}(\xi)|) \quad \text{and} \quad F(s) = \int_0^s 2\mu(\sigma)\sigma\,\mathrm{d}\sigma.$$

Equation (5.1) is a physical model and is not a gradient flow system due to the presence of the convection term $\boldsymbol{u}\cdot\nabla\boldsymbol{u}$.

By using the proposed method in this article, the system (5.1) can be discretized by

$$\begin{cases} \delta_\tau \boldsymbol{u}_n - \dfrac{1}{\alpha}\Delta\boldsymbol{u}_n + \nabla p_n = \nabla\cdot A(\nabla I_\tau \boldsymbol{u}_n) - \dfrac{1}{\alpha}\Delta I_\tau \boldsymbol{u}_n & \text{in } \mathit{\Omega}, \\ \nabla \boldsymbol{u}_n = 0 & \text{in } \mathit{\Omega}, \\ \boldsymbol{u}_n = 0 & \text{on } \partial\mathit{\Omega}, \end{cases} \tag{5.2}$$

The corresponding error equation can be written as

$$\begin{cases} \delta_\tau \boldsymbol{e}_n = \nabla\cdot A(\nabla I_\tau \boldsymbol{u}(t_n)) - \nabla\cdot A(\nabla I_\tau \boldsymbol{u}_n) \\ \qquad + \dfrac{1}{\alpha}(\Delta \boldsymbol{e}_n - \Delta I_\tau \boldsymbol{e}_n) + \boldsymbol{b}_n + \boldsymbol{d}_n \\ \qquad - (I_\tau \boldsymbol{u}(t_n)\cdot\nabla I_\tau \boldsymbol{u}(t_n) - I_\tau \boldsymbol{u}_n\cdot\nabla I_\tau \boldsymbol{u}_n) - \nabla\eta_n, \\ \nabla\cdot\boldsymbol{e}_n = 0. \end{cases} \tag{5.3}$$

where $\boldsymbol{e}_n = \boldsymbol{u}(t_n) - \boldsymbol{u}_n$ and η_n denotes the error for the pressure p at time level t_n, and $\boldsymbol{b}_n$ and $\boldsymbol{d}_n$ are truncation errors of the time discretization method, similarly as in (3.7). The error equation (5.3) has the same structure as (3.7), with $\kappa(\nabla I_\tau \boldsymbol{u}_n) \equiv 1$ and the highest-order term $\nabla\cdot A(\nabla\boldsymbol{u})$ satisfying assumptions (A1). The only difference is the extra term $\nabla\eta_n$ and the low-order term $I_\tau\boldsymbol{u}(t_n)\cdot\nabla I_\tau\boldsymbol{u}(t_n) - I_\tau\boldsymbol{u}_n\cdot\nabla I_\tau\boldsymbol{u}_n$.

Since $\nabla\cdot\boldsymbol{e}_n = 0$, testing the first error equation in (5.3) by $\boldsymbol{e}_n$ or $\boldsymbol{e}_n - \boldsymbol{e}_{n-1}$ (as we did in Sections 3.4 and 3.5) would eliminate the extra term $\nabla\eta_n$. Since the low-order term does not affect the convergence analysis, and the standard H^3 estimate for elliptic equations used in this article also holds for the Stokes problem, it follows that the error analysis in this article is applicable to the error equation (5.3) of the generalized Newtonian fluid problem.

5.2. A nonlinear parabolic system of non-divergence form. The re-parameterized mean curvature flow studied by Elliott and Fritz is described by the equation (cf. [8, with $\alpha = 1$ in Theorem 2.3])

$$\frac{\partial\boldsymbol{u}}{\partial t} = g^{ij}(\nabla\boldsymbol{u})\left(\frac{\partial^2\boldsymbol{u}}{\partial x_i\partial x_j} - \Gamma(G)^k_{ij}\frac{\partial\boldsymbol{u}}{\partial x_k}\right) \qquad (x,t)\in\Omega\times(0,T], \tag{5.4}$$

where (g^{ij}) is the inverse of a positive definite 2×2 matrix (g_{ij}) — the Riemannian metric on the surface described by the function $\boldsymbol{u} : \Omega \to \mathbb{R}^3$, with

$$g_{ij} = g_{ij}(\nabla \boldsymbol{u}) = \frac{\partial \boldsymbol{u}}{\partial x_i} \cdot \frac{\partial \boldsymbol{u}}{\partial x_j} \quad \text{for} \quad i, j = 1, 2,$$

and $\Gamma(G)_{ij}^k$, $i, j, k = 1, 2$, are given functions determined by the Riemannian metric G of the initial surface $\boldsymbol{u}_0$.

It is proved by Elliott and Fritz [8] that equation (5.4) describes the evolution of a surface which, after a hidden re-parametrization (which does not change the shape of the surface), coincides with the gradient flow of the area functional

$$E[\boldsymbol{u}] = \int_\Omega |\partial_{x_1} \boldsymbol{u} \times \partial_{x_2} \boldsymbol{u}| \mathrm{d}x,$$

where $|\partial_{x_1} \boldsymbol{u} \times \partial_{x_2} \boldsymbol{u}|$ denotes the length of the vector $\partial_{x_1} \boldsymbol{u} \times \partial_{x_2} \boldsymbol{u}$. However, equation (5.4) itself is not a gradient flow system and cannot be written into the divergence form of (1.7).

Time discretization of (5.4) by the proposed stabilization method in this article can be written as

$$\delta_\tau \boldsymbol{u}_n = g^{ij}(\nabla I_\tau \boldsymbol{u}_n) \frac{\partial^2 I_\tau \boldsymbol{u}_n}{\partial x_i \partial x_j} - \Gamma(G)_{ij}^k g^{ij}(\nabla I_\tau \boldsymbol{u}_n) \frac{\partial I_\tau \boldsymbol{u}_n}{\partial x_k} + \frac{1}{\alpha} \big(\Delta \boldsymbol{u}_n - \Delta I_\tau \boldsymbol{u}_n \big) \tag{5.5}$$

The error equation of this method can be written into the divergence form as

$$\begin{aligned} \delta_\tau \boldsymbol{e}_n = & \frac{\partial}{\partial x_i} \left(g^{ij}(\nabla \boldsymbol{u}(t_n)) \frac{\partial I_\tau \boldsymbol{e}_n}{\partial x_j} \right) + \frac{1}{\alpha} \big(\Delta \boldsymbol{e}_n - \Delta I_\tau \boldsymbol{e}_n \big) \\ & - \frac{\partial g^{ij}(\nabla \boldsymbol{u}(t_n))}{\partial x_i} \frac{\partial I_\tau \boldsymbol{e}_n}{\partial x_j} + (g^{ij}(\nabla \boldsymbol{u}(t_n)) - g^{ij}(\nabla I_\tau \boldsymbol{u}_n)) \frac{\partial^2 I_\tau \boldsymbol{u}_n}{\partial x_i \partial x_j} \\ & - \Gamma(G)_{ij}^k \left(g^{ij}(\nabla \boldsymbol{u}(t_n)) \frac{\partial \boldsymbol{u}(t_n)}{\partial x_k} - g^{ij}(\nabla I_\tau \boldsymbol{u}_n) \frac{\partial I_\tau \boldsymbol{u}_n}{\partial x_k} \right) + \boldsymbol{b}_n + \boldsymbol{d}_n. \end{aligned} \tag{5.6}$$

where $\boldsymbol{b}_n$ and $\boldsymbol{d}_n$ are the truncation errors of the time discretization method. Although the original equation (5.4) is in the non-divergence form, we see that the error equation (5.6) has the same structure as (3.7), consisting of a second-order derivative term

$$\frac{\partial}{\partial x_i} \left(g^{ij}(\nabla \boldsymbol{u}(t_n)) \frac{\partial I_\tau \boldsymbol{e}_n}{\partial x_j} \right) \quad \text{with a positive definite matrix } g^{ij}(\nabla \boldsymbol{u}(t_n)),$$

a stabilization term $\frac{1}{\alpha} \big(\Delta \boldsymbol{e}_n - \Delta I_\tau \boldsymbol{e}_n \big)$, and low-order terms which depend on $\nabla \boldsymbol{e}_n$ instead of $\nabla^2 \boldsymbol{e}_n$. Hence, the convergence analysis in this article is applicable to the time-stepping method (5.5) for the non-divergence problem (5.4). However, efficient spatial discretization for the non-divergence problem (5.4) is still challenging.

6. Numerical Examples. In this section, we provide numerical examples to support our theoretical analysis on the second-order convergence of the proposed method. We employ the finite element method using the Lagrange P2 element for spatial discretization with a sufficiently small mesh size so that the error due to spatial discretization can be neglected in observing the convergence order with respect to time stepsizes.

Example 6.1 (Mean curvature flow of graphs). We apply the method (1.10) to the equation (1.4) in the domain

$$\Omega = \{x = (x_1, x_2) : x_1^2 + x_2^2 < 1\},$$

with the initial value $u_0(x) = 2(1 - x_1^2 - x_2^2)$. The numerical solution is plotted in Figure 6.1, which shows the evolution of the 2D surface described by the graph $\{(x, u(x,t)) : x \in \Omega\}$.

For a fixed discretization of Ω with mesh size $h = 7.75 \times 10^{-3}$, we present the relative errors of numerical solutions for different time stepsizes in Table 6.1, with

$$\text{relative error} := \frac{\|u(T) - u_N\|_{L^2}}{\|u(T)\|_{L^2}},$$

where $u(T)$ is given by a reference solution from using a smaller stepsize $\tau = 2 \times 10^{-4}$. The numerical results indicate that the errors are $O(\tau^2)$, which is consistent with our theoretical analysis.

TABLE 6.1
Example 6.1: Errors of numerical solutions at $T = 0.1$

τ	relative error	rate
5.00e-3	4.93e-3	–
2.50e-3	1.29e-3	1.93
1.25e-3	3.57e-4	1.86
6.25e-4	7.79e-5	2.20

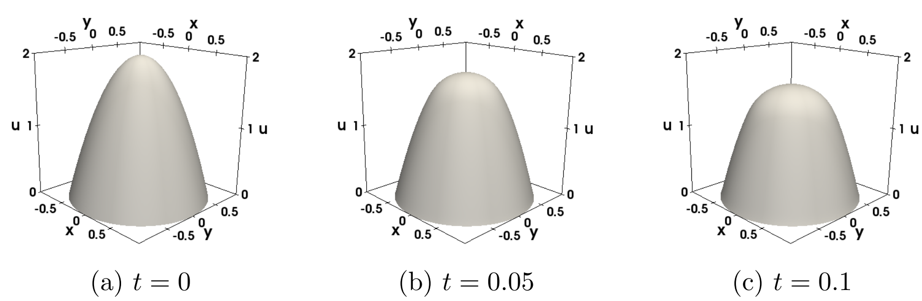

Fig. 6.1. *Example 6.1: The mean curvature flow of graphs*

Example 6.2 (Re-parameterized curve shortening flow). We apply the method (1.10) to compute to the equation (1.5), with the initial value

$$\boldsymbol{u}_0 := ((2 + 0.5\cos(s))\cos(2s), (2 + 0.5\cos(s))\sin(2s)).$$

The numerical solutions are plotted as 2D closed curves in Figure 6.2.

The initial curve has a self-intersection at point $(-2, 0)$ $(s = \frac{\pi}{2}, \frac{3}{2})$. In view of Figure 6.2, the wind shrinks to the intersecting point and then disappears resulting a cusp (singularity) near $t = 1.547$, where the curvature becomes ∞ and causes the

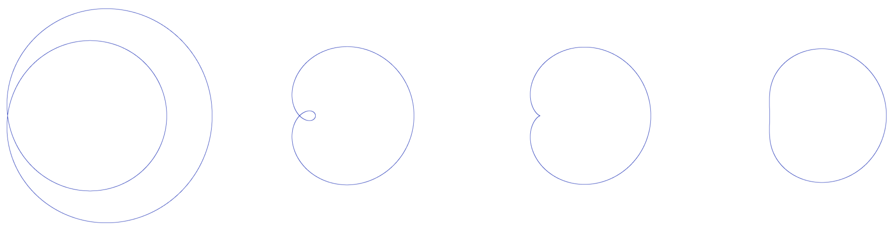

(a) $t = 0$ (b) $t = 1.533$ (c) $t = 1.547$ (d) $t = 1.6$

Fig. 6.2. *Example 6.2: Re-parameterized curve shortening flow:* $\boldsymbol{u}_0$ *has one self-intersection*

regularity lost of $\boldsymbol{u}$. In Figure 6.3, we plot $\boldsymbol{u} = (u_1(s), u_2(s))$ as functions on $[0, 2\pi]$ at $t = 1.547$. The inner wind shrinking to a point means that $\boldsymbol{u}(s)$ becomes a constant (i.e., $|\frac{\partial \boldsymbol{u}}{\partial s}| = 0$) at some subinterval of $[0, 2\pi]$.

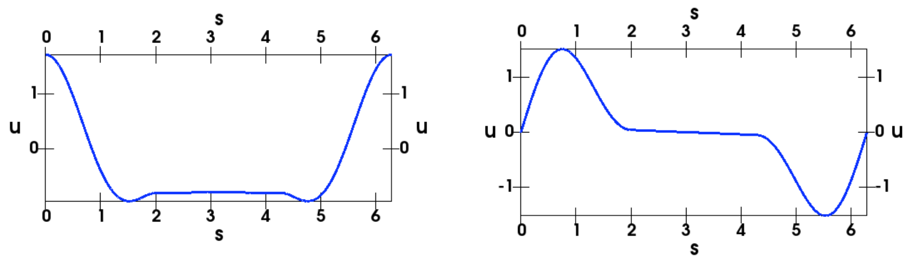

(a) $u_1, \ t = 1.547$ (b) $u_2, \ t = 1.547$

Fig. 6.3. *Example 6.2: Re-parameterized curve shortening flow:* $\boldsymbol{u}_0$ *has one self-intersection.* $\boldsymbol{u} = (u_1(s), u_2(s))$ *at* $t = 1.556$, $s \in [0, 2\pi]$.

For a fixed discretization of $[0, 2\pi]$ with mesh size $h = \frac{\pi}{1000}$, we change the time-step increment τ and compute the relative error $:= \frac{\|\boldsymbol{u}(T) - \boldsymbol{u}_N\|_{L^2}}{\|\boldsymbol{u}(T)\|_{L^2}}$, where $u(T)$ is given by a reference solution from using a smaller stepsize $\tau = T/3000$. We intend to investigate the convergence order before and after the self-intersection disappears respectively. To this end, we present the errors of numerical solutions in Table 6.2 and Table 6.3 for $T = 1$ and $T = 1.6$, respectively.

The numerical results show that the method is second-order convergent at $T = 1$ before the inner wind shrinks to a point. This is consistent with our theoretical analysis. However, the method is only first-order convergent at $T = 1.6$ due to the regularity lost when the wind shrinks to one point. Convergence analysis in this case is beyond the assumptions made in this article and remains challenging.

Furthermore, we test (1.10) for an initial curve

$$\boldsymbol{u}_0 = (2 + \cos(s))(\cos(5s) + \cos(s) + \sin(s), \sin(5s) + \sin(s))$$

with multiple self-intersections. The curve evolution is presented in Figure 6.4, where we can see that all the inner winds shrink successively to singular points with ∞-curvature. Numerically we can still observe first-order convergence at $T = 4$; see Table 6.4. This is beyond our theoretical analysis.

Table 6.2

Example 6.2: Errors at $T = 1$ (before inner wind shrinks to a point)

τ	relative error	rate
2.50e-2	2.25e-3	–
1.25e-2	5.75e-3	1.97
6.25e-3	1.45e-4	1.99
3.13e-3	3.62e-4	2.00
1.56e-3	8.75e-5	2.05

Table 6.3

Example 6.2: Errors at $T = 1.6$ (after inner wind shrinks to a point)

τ	relative error	rate
4.00e-2	2.39e-1	–
2.00e-2	1.24e-1	0.94
1.00e-3	4.61e-2	1.43
5.00e-3	2.30e-2	1.00
2.50e-3	1.17e-3	0.97

Finally, we compute the curve shortening flow for an initial curve

$$\boldsymbol{u}_0 = (\cos(s), \sin(s) + \cos^{\frac{2}{3}}(s))$$

with cusps; see Figure 6.5 (a). The cusps disappear immediately, as shown in Figure 6.5. The error in Table 6.5 indicates that the method has first-order convergence at $T = 0.2$. This is beyond our theoretical analysis. The convergence analysis for an initial curve with cusps is challenging and remains open.

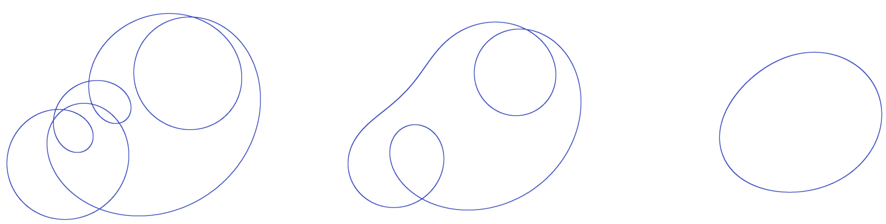

$t = 0$ $t = 1$ $t = 4$

Fig. 6.4. *Example 6.2: $\boldsymbol{u}_0$ has several winds*

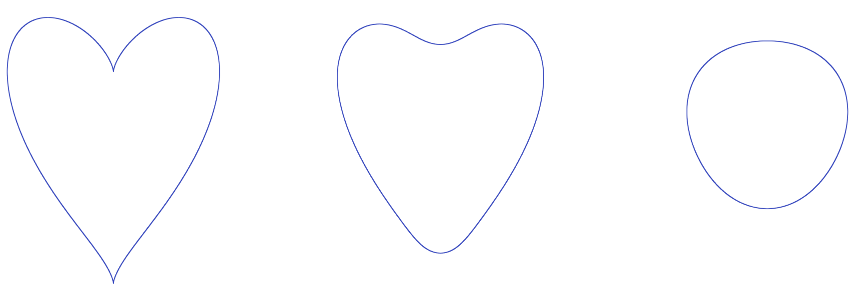

$t = 0$ $t = 0.05$ $t = 0.2$

Fig. 6.5. *Example 6.2: $\boldsymbol{u}_0$ has two cusps*

Example 6.3 (Mean curvature flow of parametric surface). In this last example, we consider the mean curvature flow of parametric surfaces described by the

Table 6.4
Example 6.2: The errors at $T = 4$ when $\boldsymbol{u}_0$ has several winds

τ	relative error	rate
2.50e-2	1.40e-2	–
1.25e-2	8.90e-3	0.67
6.25e-3	4.86e-3	0.87
3.13e-3	2.07e-3	1.22

Table 6.5
Example 6.2: Errors at $T = 0.2$ when $\boldsymbol{u}_0$ has cusps

τ	relative error	rate
2.50-3	1.46e-2	–
1.25e-3	8.36e-3	0.80
6.25e-4	4.55e-3	0.88
3.13e-4	2.26e-3	1.01

evolution equation (cf. [6, §4])

$$\sqrt{|\det(g_{ij})|}\,\frac{\partial \boldsymbol{u}}{\partial t} = \frac{\partial}{\partial x_i}\left(\sqrt{|\det(g_{ij})|}\,g^{ij}\,\frac{\partial \boldsymbol{u}}{\partial x_j}\right), \tag{6.1}$$

where (g^{ij}) is the inverse matrix of the 2×2 matrix (g_{ij}) (the Riemannian metric on the surface described by the function $\boldsymbol{u} : \Omega \to \mathbb{R}^3$), with

$$g_{ij} = \frac{\partial \boldsymbol{u}}{\partial x_i} \cdot \frac{\partial \boldsymbol{u}}{\partial x_j} \quad \text{for} \quad i, j = 1, 2.$$

This is the gradient flow of the area functional

$$E[\boldsymbol{u}] = \int_\Omega |\partial_{x_1}\boldsymbol{u} \times \partial_{x_2}\boldsymbol{u}|\mathrm{d}x,$$

where $|\cdot|$ denotes the length of the vector $\partial_{x_1}\boldsymbol{u} \times \partial_{x_2}\boldsymbol{u}$.

Equation (6.1) is strongly parabolic. However, it does not have the local positivity property (P2). In this case, we investigate the convergence of numerical solutions given by the proposed method (6.1) to test the effectiveness of the proposed method beyond the assumptions in this article.

We set $\Omega = \{x = (x_1, x_2) : x_1^2 + x_1^2 < 1\}$ and the initial value

$$\boldsymbol{u}(x,t)|_{t=0} = \boldsymbol{u}_0 := (x_1, x_2, 2(1 - x_1^2 - x_2^2) + x_1^2) \in \mathbb{R}^3. \tag{6.2}$$

The boundary of the initial surface $\boldsymbol{u}_0$ is homeomorphic to $\partial\Omega := \{(x_1, x_2, 0) \mid x_1^2 + x_2^2 = 1\} \subset \mathbb{R}^3$. The boundary condition for the mean curvature flow is imposed by

$$\boldsymbol{u}(t) = \boldsymbol{u}_0 \quad \text{on } \partial\Omega \times [0, T],$$

which means the surface $\boldsymbol{u}(x,t)$ has a fixed closed boundary $\Gamma := \{(x_1, x_2, x_3) \mid x_1^2 + x_2^2 = 1,\ x_3 = x_1^2\}$. In numerical simulation, Ω is discretized by a triangulation with mesh size $h = 3.13 \times 10^{-2}$, and the finite element method is applied. The motion of the parametric surface $\boldsymbol{u}(x,t) \subset \mathbb{R}^3$ is plotted in Figure 6.6, which tends to the minimal surface (a saddle surface). Moreover, we list the relative error $:= \frac{\|\boldsymbol{u}(T) - \boldsymbol{u}_N\|_{L^2}}{\|\boldsymbol{u}(T)\|_{L^2}}$ for different time stepsizes in Table 6.6, with a reference solution $u(T)$ computed from using stepsize $\tau = 5.00 \times 10^{-4}$. The numerical results elucidate the convergence rate $O(\tau^2)$.

The proposed method is also applicable to the mean curvature flow which develop singularity (thus blow up) in finite time. We adopt the same domain and boundary

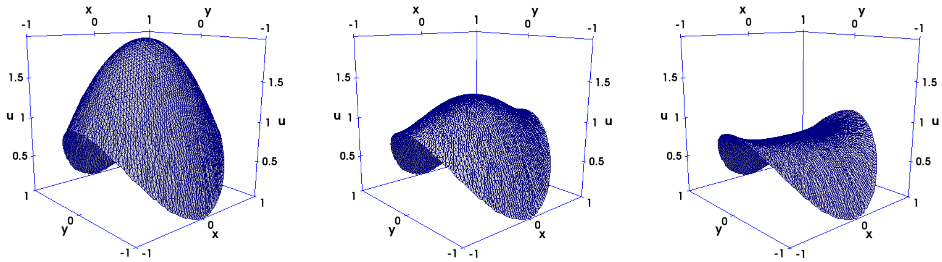

$t = 0$ $t = 0.16$ $t = 0.4$

Fig. 6.6. *Example 6.3(i): Mean curvature flow of parametric surfaces*

Table 6.6
Example 6.3(i): Errors at $T = 0.2$ for mean curvature flow of parametric surfaces

τ	relative error	rate
1.00e-2	6.44e-2	–
5.00e-3	1.61e-2	2.00
2.50e-3	3.29e-3	2.29
1.25e-3	7.39e-4	2.15

condition to the previous example, but replace the initial value (6.2) by a dumbbell shaped surface

$$\boldsymbol{u}_0 = (R(x_1, x_2)x_1, R(x_1, x_2)x_2, 10(1 - x_1^2 - x_2^2)),$$

where $R(x_1, x_2) = (\cos(\frac{7\pi}{4}(x_1^2+x_2^2))+1.4)\log(4.3-3(x_1^2+x_2^2))/(\log(1.3)(\cos\frac{7\pi}{4}+1.4))$. The evolution of the surface is plotted in Figure 6.7, where we take small stepsize $\tau = 3 \times 10^{-5}$ to capture the singularity.

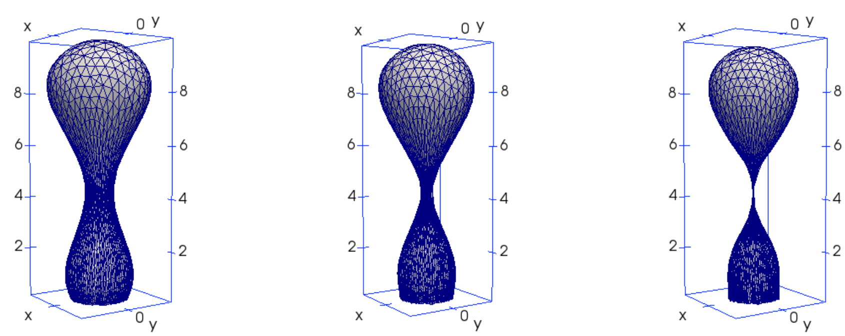

$t = 0$ $t = 0.15$ $t = 0.2475$

Fig. 6.7. *Example 6.3(ii): Mean curvature flow with dumbbell shaped initial surface*

When the solution is smooth, as in Figure 6.6, we have not observed any coupling condition between τ and h. However, in the numerical simulation in Figure 6.7, we observed that a grid-ratio condition $\tau = h^2$ is needed to capture the singularity. Error analysis in the presence of singularity is still challenging and open questions in the field of numerical approximation to geometric curvature flows.

Appendix: Regularity results of complex-valued elliptic equations

Let $a_{ij} \in L^\infty(\Omega;\mathbb{C})$ be complex-valued functions satisfying the following ellipticity condition:

$$\lambda^{-1}\sum_{j=1}^{d}|\xi_j|^2 \le \mathrm{Re}\sum_{i,j=1}^{d} a_{ij}(x)\xi_i\xi_j \le \lambda\sum_{j=1}^{d}|\xi_j|^2, \quad \forall\, x\in\Omega \quad \text{and} \quad \forall\, \xi_j \in \mathbb{C},\ j=1,\dots,d, \tag{A.1}$$

where λ is a fixed positive constant. Consider the following problem:

$$\begin{cases} \partial_i(a_{ij}\partial_j u) = f & \text{in } \Omega, \\ u = 0 & \text{on } \partial\Omega. \end{cases} \tag{A.2}$$

Proposition A *If $a_{ij} \in W^{s,\infty}(\Omega;\mathbb{C})$ and $f \in H^{s-1}(\Omega;\mathbb{C})$, then* (A.2) *has a unique solution $u \in H^{s+1}(\Omega;\mathbb{C})$, and*

$$\|u\|_{H^{s+1}(\Omega;\mathbb{C})} \le C\|f\|_{H^{s-1}(\Omega;\mathbb{C})} \quad \text{for } s=0,1,2.$$

Proof. Let $b_{ij} = \mathrm{Re}(a_{ij})$ and $c_{ij} = \mathrm{Im}(a_{ij})$, and let $u = u_1 + iu_2$, with real-valued functions u_1 and u_2. Then (A.2) is equivalent to

$$\begin{cases} \displaystyle\sum_{k,l=1}^{d} \partial_k(b_{kl}\partial_l u_1 - c_{kl}\partial_l u_2) = \mathrm{Re}(f) & \text{in } \Omega, \\ \displaystyle -\sum_{k,l=1}^{d} \partial_k(b_{kl}\partial_l u_2 + c_{kl}\partial_l u_1) = -\mathrm{Im}(f) & \text{in } \Omega, \\ u_1 = u_2 = 0 & \text{on } \partial\Omega. \end{cases} \tag{A.3}$$

This system of equations can be further written as

$$\begin{cases} \displaystyle\sum_{k,l=1}^{d}\sum_{j=1}^{2} \partial_k(B_{k1,lj}\partial_l u_j) = \mathrm{Re}(f) & \text{in } \Omega, \\ \displaystyle\sum_{k,l=1}^{d}\sum_{j=1}^{2} \partial_k(B_{k2,lj}\partial_l u_j) = \mathrm{Im}(f) & \text{in } \Omega, \\ u_1 = u_2 = 0 & \text{on } \partial\Omega. \end{cases} \tag{A.4}$$

with

$$B_{k1,l1} = b_{kl}, \quad B_{k1,l2} = -c_{kl}, \quad B_{k2,l1} = -c_{kl}, \quad B_{k2,l2} = -b_{kl}. \tag{A.5}$$

The coefficients $B_{kp,lq}$ satisfy the following identity: for $\xi_{lq} \in \mathbb{R}$ there holds

$$\begin{aligned} \sum_{k,l=1}^{d}\sum_{p,q=1}^{2} B_{kp,lq}\xi_{lq}\xi_{kp} &= \sum_{k,l=1}^{d}\sum_{p,q=1}^{2} \big(b_{kl}\xi_{l1}\xi_{k1} - c_{kl}\xi_{l2}\xi_{k1} - c_{kl}\xi_{l1}\xi_{k2} - b_{kl}\xi_{l2}\xi_{k2}\big) \\ &= \sum_{k,l=1}^{d} \big[(b_{kl}\xi_{l1} - c_{kl}\xi_{l2})\xi_{k1} - (c_{kl}\xi_{l1} + b_{kl}\xi_{l2})\xi_{k2}\big] \end{aligned}$$

$$= \sum_{k,l=1}^{d} \left[\mathrm{Re}(a_{kl}\xi_l)\mathrm{Re}(\xi_k) - \mathrm{Im}(a_{kl}\xi_l)\mathrm{Im}(\xi_k) \right]$$

$$= \mathrm{Re} \sum_{k,l=1}^{d} a_{kl}\xi_l\xi_k.$$

Therefore, the complex ellipticity condition (A.1) is equivalent to

$$\lambda^{-1} \sum_{k=1}^{d} \sum_{p=1}^{2} |\xi_{kp}|^2 \le \sum_{k,l=1}^{d} \sum_{p,q=1}^{2} B_{kp,lq}\xi_{lq}\xi_{kp} \le \lambda \sum_{k=1}^{d} \sum_{p=1}^{2} |\xi_{kp}|^2, \quad \forall\, \xi_{kp} \in \mathbb{R}, \qquad \text{(A.6)}$$

which is exactly the real-valued ellipticity condition for system of equations.

If $B_{kp,lq} \in W^{s,\infty}(\Omega)$ then [11, Theorem 4.14] implies that (A.4) has a unique solution $(u_1, u_2) \in H^{s+1}(\Omega) \times H^{s+1}(\Omega)$. Equivalently, if $a_{ij} \in W^{s,\infty}(\Omega; \mathbb{C})$ then the above argument implies that (A.2) has a unique solution $u \in H^{s+1}(\Omega; \mathbb{C})$. □

REFERENCES

[1] G. Akrivis: Stability of implicit-explicit backward difference formulas for nonlinear parabolic equations. *SIAM J. Numer. Anal.* 53 (2015), pp. 464–484.

[2] G. Akrivis and C. Lubich: Fully implicit, linearly implicit and implicit–explicit backward difference formulae for quasi-linear parabolic equations. *Numer. Math.* 131 (2015), pp. 713–735.

[3] L. Chen: Phase-field models for microstructure evolution. *Annu. Rev. Mater. Res.* 32 (2002), pp. 113–140.

[4] C. Cheng, V. Thomée, and L. Wahlbin: Finite element approximation of a parabolic integro-differential equation with a weakly singular kernel. *Math. Comp.* 58 (1992), pp. 587–602.

[5] K. Deckelnick and G. Dziuk: On the approximation of the curve shortening flow. *Calculus of Variations, Applications and Computations*, (1994) pp. 100–108. Pont-à-Mousson, Pitman Research Notes in Mathematics Series, Harlow: Longman Scientific & Technical.

[6] K. Deckelnick, G. Dziuk, and C. M. Elliott: Computation of geometric partial differential equations and mean curvature flow. *Acta Numerica* 14 (2005), pp. 139–232.

[7] M. Droske and M. Rumpf: A level set formulation for Willmore flow. *Interfaces and free boundaries* 6 (2004), pp. 361–378.

[8] C. M. Elliott and H. Fritz: On approximations of the curve shortening flow and of the mean curvature flow based on the DeTurck trick. *IMA J. Numer. Anal.* 37 (2017), pp. 543–603.

[9] M. Fathi: A gradient flow approach to large deviations for diffusion processes. *Journal de Mathématiques Pures et Appliquées* 106 (2016), pp. 957–993.

[10] X. Feng and A. Prohl: Analysis of total variation flow and its finite element approximations. *Math. Mod. Num. Analysis* 37 (2003), pp. 533–556.

[11] M. Giaquinta and L. Martinazzi: An introduction to the regularity theory for elliptic systems, harmonic maps and minimal graphs. *Lecture Notes. Scuola Normale Superiore di Pisa* 11. Edizioni della Normale, Pisa, Second edition, 2012.

[12] J. G. Heywood and R. Rannacher: Finite element approximation of the nonstationary Navier-Stokes problem IV: Error analysis for second-order time discretization. *SIAM J. Numer. Anal.* 27 (1990), pp. 353–384.

[13] G. Huisken: Non-parametric mean curvature evolution with boundary conditions. *J. Differ. Equations* 77 (1989), pp. 369–378.

[14] W. Kern and B. U. Felderhof: *Variational principle for flow of generalized Newtonian fluids.* Z. Physik B 29 (1978), pp. 293–297.

[15] P. C. Kunstmann, B. Li, and C. Lubich: Runge-Kutta time discretization of nonlinear parabolic equations studied via discrete maximal parabolic regularity. *Found. Comput. Math.* 18 (2018), pp. 1109–1130.

[16] B. Li and W. Sun: Error analysis of linearized semi-implicit Galerkin finite element methods for nonlinear parabolic equations. *Int. J. Numer. Anal. & Modeling* 10 (2013), pp. 622–633.

[17] B. Li and W. Sun: Linearized FE approximations to a nonlinear gradient flow. *SIAM J. Numer. Anal.* 52 (2014), pp. 2623–2646.

[18] S. Lisini: Nonlinear diffusion equations with variable coefficients as gradient flows in Wasserstein spaces. *ESAIM: Control, Optimisation and Calculus of Variations* 15 (2009), pp. 712–740.

[19] J. Liu: Simple and efficient ALE methods with provable temporal accuracy up to fifth order for the stokes equations on time varying domains. *SIAM J. Numer. Anal.* 51 (2013), pp. 743–772.
[20] C. Lubich: On the convergence of multistep methods for nonlinear stiff differential equations. *Numer. Math.* 58 (1990), pp. 839–853.
[21] C. Lubich and A. Ostermann: Runge-Kutta approximation of quasi-linear parabolic equations. *Math. Comp.* 64 (1995), pp. 601–627.
[22] H. Murakawa: A linear finite volume method for nonlinear cross-diffusion systems. *Numer. Math.* 136 (2017), pp. 1–26.
[23] O. Michailovich, Y. Rathi, and A. Tannenbaum: Image segmentation using active contours driven by the Bhattacharyya gradient flow. *IEEE Trans. Image Process.* 16 (2007), pp. 2787–2801.
[24] A. Ostermann and M. Thalhammer: Convergence of Runge–Kutta methods for nonlinear parabolic equations. *Appl. Numer. Math.* 42 (2002), pp. 367–380.
[25] F. Otto: The geometry of dissipative evolution equations: the porous medium equation. *Comm. Partial Differential Equations* 26 (2001), pp. 101–174.
[26] J. Prüss and G. Simonett: Moving Interfaces and Quasilinear Parabolic Evolution Equations. Birkhäuser, Switzerland, 2016.
[27] L. Rudin, S. Osher, and E. Fatemi: Nonlinear total variation based noise removal algorithms. *Physica D: Nonlinear Phenomena* 60 (1992), pp. 259–268.
[28] M. Rumpf and O. Vantzos: Numerical gradient flow discretiza- tion of viscous thin films on curved geometries. *Math. Models Methods Appl. Sci.* 23 (2013), pp. 917–947.
[29] F. Santambrogio: *Optimal Transport for Applied Mathematicians: Calculus of Variations, PDEs, and Modeling.* Progress in Nonlinear Differential Equations and Their Applications. Springer International Publishing, 2015.
[30] J. Shen and J. Xu: Convergence and error analysis for the scalar auxiliary variable (SAV) schemes to gradient flows. *SIAM J. Numer. Anal.* 56 (2018), pp. 2895–2912.
[31] R. Strzodka, M. Droske, and M. Rumpf: Image registration by a regularized gradient flow. A streaming implementation in DX9 graphics hardware. *Computing* 73 (2004), pp. 373–389.
[32] J. L. Vazquez: *The Porous Medium Equation: Mathematical Theory.* Oxford Mathematical Monographs. Clarendon Press, 2007.
[33] C. Villani: *Topics in Optimal Transportation.* Graduate studies in mathematics. American Mathematical Society, 2003.